Structure and Function of the Phosphothreonine-Specific FHA Domain
Anjali Mahajan, Chunhua Yuan, Hyun Lee, Eric S.-W. Chen, Pei-Yu Wu and Ming-Daw Tsai (23 December 2008)
Science Signaling **1** (51), re12. [DOI: 10.1126/scisignal.151re12]

Science Signaling (ISSN 1937-9145) is published weekly, except the last week in December, by the American Association for the Advancement of Science, 1200 New York Avenue, NW, Washington, DC 20005.

BIOCHEMISTRY

Structure and Function of the Phosphothreonine-Specific FHA Domain

Anjali Mahajan,[1] Chunhua Yuan,[2] Hyun Lee,[1,3] Eric S.-W. Chen,[3,4,5] Pei-Yu Wu,[5] Ming-Daw Tsai[1,2,3,4,5*]

Published 23 December 2008; Volume 1 Issue 51, re12; Revised 17 February 2009

The forkhead-associated (FHA) domain is the only known phosphoprotein-binding domain that specifically recognizes phosphothreonine (pThr) residues, distinguishing them from phosphoserine (pSer) residues. In contrast to its very strict specificity toward pThr, the FHA domain recognizes very diverse patterns in the residues surrounding the pThr residue. For example, the FHA domain of Ki67, a protein associated with cellular proliferation, binds to an extended target surface involving residues remote from the pThr, whereas the FHA domain of Dun1, a DNA damage–response kinase, specifically recognizes a doubly phosphorylated Thr-Gln (TQ) cluster by virtue of its possessing two pThr-binding sites. The FHA domain exists in various proteins with diverse functions and is particularly prevalent among proteins involved in the DNA damage response. Despite a very short history, a number of unique structural and functional properties of the FHA domain have been uncovered. This review highlights the diversity of biological functions of the FHA domain–containing proteins and the structural bases for the novel binding specificities and multiple binding modes of FHA domains.

Introduction

The forkhead-associated (FHA) domain, a protein-phosphoprotein interaction motif with high specificity for phosphothreonine (pThr) residues, has been identified in more than 2000 proteins (from the Pfam database) in prokaryotes and eukaryotes since its discovery in forkhead family transcription factors in 1995 (*1*). It is present in many regulatory proteins, kinases, phosphatases, and transcription factors (*1*) (Fig. 1A). It is now clear that FHA domains play important roles in human diseases, particularly in relation to DNA damage responses and cancers, and in biological processes such as cell growth, signal transduction, and cell cycle regulation (Fig. 2). Specific roles for FHA domains in checkpoint pathways have been explored with regard to various kinases in different species (Fig. 1B). Some examples of FHA domain–containing proteins include the human tumor suppressor checkpoint kinase 2 (Chk2), checkpoint with forkhead and ring finger domains (CHFR) (*2*), TIFA [tumor necrosis factor receptor (TNFR)–associated factor (TRAF)–interacting protein with a forkhead-associated domain] (*3*), and Nijmegen breakage syndrome 1 (NBS1, also known as nibrin) (*4*).

The FHA domain is unique among signal transduction domains in two aspects. First, it is the only presently known protein domain that specifically recognizes pThr; other domains such as WW and 14-3-3 recognize both pThr and pSer residues. Second, the FHA domain shows very diverse ligand specificity; different FHA domains recognize the pTXXD motif, the pTXXI/L motif, and TQ clusters (singly and multiply phosphorylated) (*5*). The Ki67-FHA even recognizes an extended binding surface, but not short phosphopeptides. Here, we discuss FHA domains in terms of their structure, binding specificity, and biological function, and we highlight multiple binding modes, possible alternative binding sites, and their importance in providing diversity to their functions in regulating multiple signaling pathways. Although the FHA domain has been known for only a relatively short period of time, a great deal of information has already been acquired, particularly since it was last reviewed in 2002 by Durocher and Jackson (*6*) and in 2003 by Heierhorst and colleagues (*7*).

[1]Biophysics Program, Ohio State University, Columbus, OH 43210, USA. [2]Campus Chemical Instrument Center, Ohio State University, Columbus, OH 43210, USA. [3]Genomics Research Center, Academia Sinica, Taipei 115, Taiwan. [4]Institute of Biochemical Science, National Taiwan University, Taipei 10617, Taiwan. [5]Institute of Biological Chemistry, Academia Sinica, Taipei 115, Taiwan.

*Corresponding author. E-mail: mdtsai@gate.sinica.edu.tw

Structures of Free FHA Domains

To date, the structures of 16 FHA domains have been determined either in their free forms, in complexes with ligand, or both, by nuclear magnetic resonance (NMR) and x-ray crystallography studies (http://www.rcsb.org) (Table 1). The first reported structure is the C-terminal FHA domain of the protein Rad53 identified from radiosensitive mutants of budding yeast, Rad53-FHA2, which was solved by NMR (*8*) (Fig. 3). Consistent with proteolytic digestion studies (*9*), all structures clearly show that the FHA domain is considerably larger than the 55 to 75 amino acid residues—the core FHA domain homology region—predicted by sequence analyses (*1*). The minimal structure of an FHA domain encompasses the essential 11 β strands and spans approximately from 95 residues (in the case of Ki67-FHA) to 121 residues (in the case of Rad53-FHA2). Although some N-terminal or C-terminal flanking sequences are often needed to obtain soluble and stable proteins, an FHA domain construct is still generally under 150 residues, which makes it well suited for structural determination by solution NMR studies.

The FHA domain is typically characterized by the following features (Fig. 3): (i) It is rich in β strands; there are 11 more or less well-defined β strands numbered from β1 to β11. (ii) It consists of two large β sheets. One sheet contains six antiparallel strands (β2, β1, β11, β10, β7, and β8); the other sheet contains five mixed β strands (β4, β3, β5, β6, and β9), of which β4 is the shortest and is parallel to β3. (iii) It contains a twisted β sandwich; this is the core architecture of the tertiary fold formed by burying hydrophobic side chains between the two large β sheets. (iv) It has structural modularity; the first and last β strands intimately interact with each other as part of one piece of the β sandwich, and the N terminus and C terminus meet at the end of the domain opposite to the pThr-binding site (Fig. 3). In conclusion, despite sharing low sequence homology, all known FHA domains adopt a strikingly similar fold, a structural feature that could be attributed to the preservation of hydrophobicity in the β strands (*10*). A structure-based sequence alignment of FHA domains is shown in Fig. 4A.

Major structural differences between different FHA domains occur in the loops and turns that connect the β strands, which can either vary substantially in length, contain a small α-helical insertion, or both. This is exemplified by comparisons between Rad53-FHA1 and Rad53-FHA2, with the former having a short helical insertion

between the β2 and β3 strands (*11*, *12*), whereas the latter has a much longer loop between the β5 and β6 strands (*8*). However, some structures determined so far show that the conserved residues located at the binding loops are positioned quite similarly in three-dimensional space. For example, despite a helical insertion in the loop between the β4 and β5 strands, the conserved Gly^{116}, Arg^{117}, Ser^{140}, and His^{143} residues of the FHA domain of Chk2 can be spatially overlaid with the corresponding residues in Rad53-FHA1 (*13*). Moreover, regardless of the exact sequence, the conserved SXXH motif ($S^{85}NKH^{88}$ in FHA1) or its variant, such as $S^{47}RNQ^{50}$ in mouse polynucleotide kinase (PNK)-FHA (*14*), forms a protruding U-turn shape preceding the β5 strand.

In the mitotic checkpoint protein CHFR, the FHA domain forms a segment-swapped dimer, in which a C-terminal segment of one molecule occupies the position of the corresponding segment of the other molecule (*15*). It remains to be established whether this swapping has any biological implications, such as in protein oligomerization. However, human Chk2 and the *Saccharomyces cerevisiae* kinase Rad53 can self-dimerize and oligomerize, and their FHA domains are indispensable for these phosphorylation-dependent events (*16*–*18*).

It is noteworthy that the structural topology of the FHA domain is similar to that of the MH2 (mothers against decapentaplegic homolog 2) domain of the tumor suppressor Smad (*11*, *19*). However, although they have an identical core β-sandwich, the MH2 domain contains several helical insertions and has a different topology of its loops compared with that of the FHA domain (*8*, *11*). Huse *et al*. proposed that the functions of these domains may also be conserved (*20*). A type I transforming growth factor–β (TGF-β) receptor–derived phosphopeptide interacts with MH2 in a region that coincides with the phosphopeptide-interaction region of FHA domains (*20*).

Combinatorial Library Approach and Ligand Specificity

The combinatorial peptide library approach was introduced in the early 1990s to study the ligand specificity of the Src homology 2 (SH2) domain (*21*) and has since been successfully applied to many protein-protein interaction domains, including the phosphotyrosine-binding (PTB) domain, WW, and 14-3-3 domains, which recognize short pThr-, pTyr-, or pSer-containing motifs (*22*). When the structure of the FHA domain was solved (*8*), its ligand specificity was not clear, despite some pioneering biological studies showing its phosphoprotein-binding role (*23*–*26*). Three types of combinatorial libraries—pThr, pSer, and pTyr—with two or three residues on each side randomized (for example, XXXpTXXX) were thus used to elucidate ligand specificity. Two laboratories, using different screening and analytical methods, independently arrived at the conclusion that Rad53-FHA1 specifically recognizes pTXXD (*11*, *12*). The specificity of Rad53-FHA2 was less certain, and both pYXL (*27*) and pTXXL (*11*, *12*) have been suggested as potential recognition motifs. Overall, the results of library screening and biological studies of several FHA domains led to the suggestion of the "pThr+3 rule" for FHA domains, with the pThr and the pThr+3 residues being the primary and secondary recognition sites, respectively, and the preferred +3 residues falling into two major categories: Asp and Ile or Leu (*11*, *28*). There are some exceptions. For example, the FHA domain of kinase-associated protein phosphatase (KAPP) prefers Ser or Ala (*11*, *29*), whereas the RING-finger protein 8 (RNF8)–FHA domain displays a strong preference for Tyr and Phe at the pThr+3 position (*30*). The results from combinatorial library screenings are summarized in Table 2.

The structures of several complexes between FHA domains and phosphopeptides obtained from library screening have been reported (Table 1). An example is the crystal structure of human Chk2-FHA in complex with the synthetic peptide "HFD(pT)YLI," which contains Ile at the pThr+3 position (Fig. 5, A and B) (*13*). In a separate study, the $pT^{68}XXL$ motif from Chk2 was also tested in vitro and shown, through NMR studies, to bind to Chk2-FHA with modest affinity (K_d of ~12.3 μM) (*31*).

The pThr-binding region in an FHA domain typically includes residues in the loops and turns between the following pairs of β strands: β3-β4, β4-β5, β6-β7, and β10-β11 (Fig. 5A). Overall, the bound peptide typically exists in an extended conformation around the pThr residue, and its binding induces little global conformational change in the FHA domain. The latter is also self-evident in two-dimensional ^{1}H-^{15}N heteronuclear single-quantum coherence (HSQC) experiments, which show relatively small changes in chemical shifts in the FHA domain upon peptide binding (*10*, *27*, *31*–*36*), for

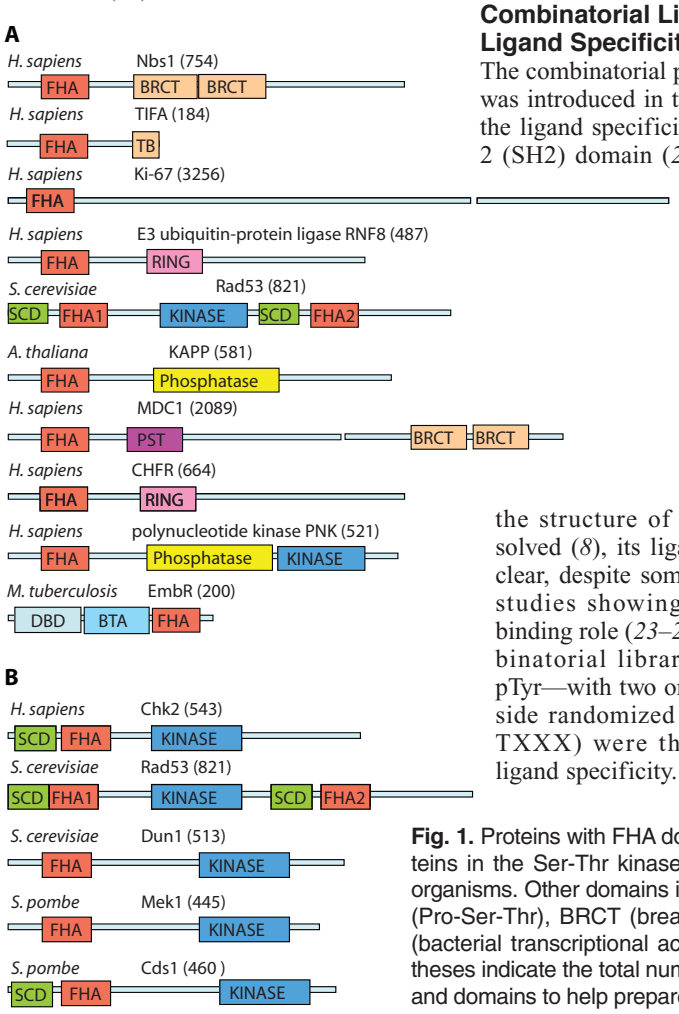

Fig. 1. Proteins with FHA domains. (**A**) Proteins with diverse functions in different organisms. (**B**) Proteins in the Ser-Thr kinase family that have functions specific to checkpoint pathways in different organisms. Other domains indicated are phosphatase, RING (ring finger), SCD (SQ-TQ cluster), PST (Pro-Ser-Thr), BRCT (breast cancer susceptibility gene–1 C-terminal), TB (TRAF6 binding), BTA (bacterial transcriptional activation), DBD (DNA-binding), and kinase domains. Numbers in parentheses indicate the total number of amino acid residues in each protein. [Information about sequences and domains to help prepare this figure was obtained from http://www.sanger.ac.uk/software/pfam/.]

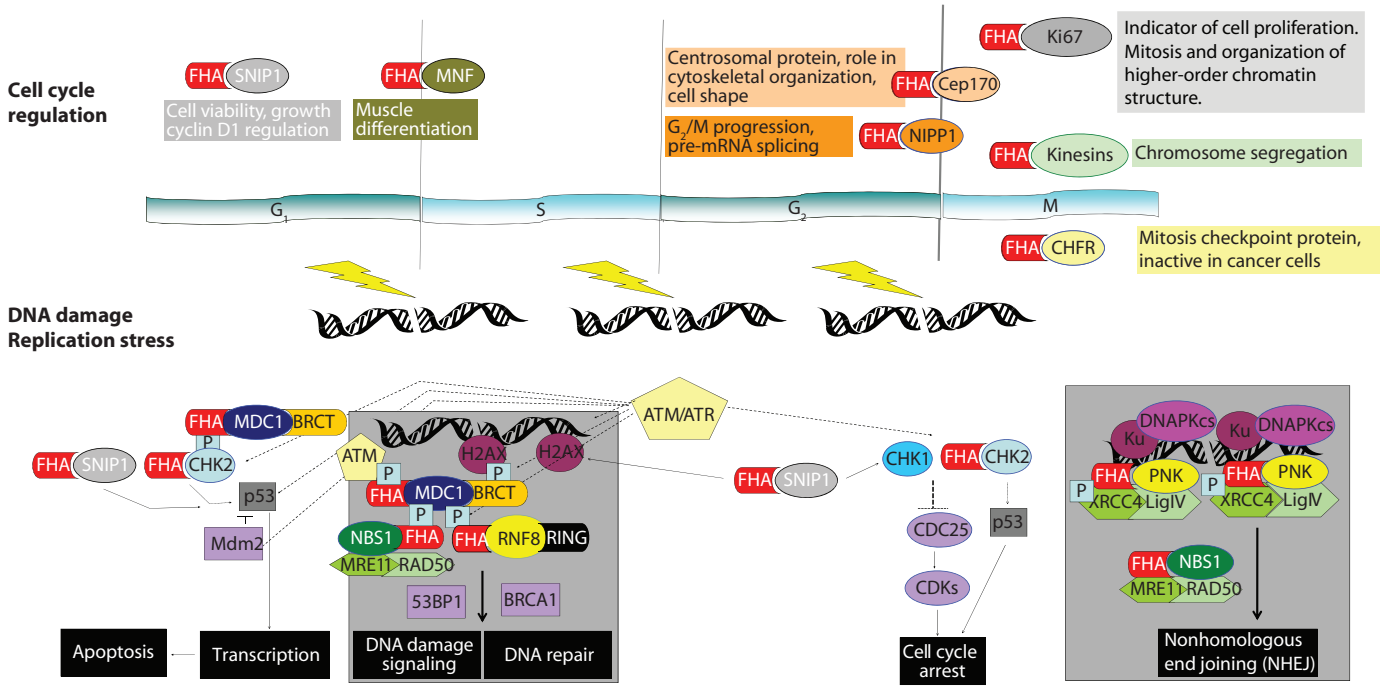

Fig. 2. Diagram of proposed functions of FHA domain–containing proteins. See main text for details.

example, Dun1 [DNA-damage uninducible (Dun) mutant 1] (Fig. 5C). However, NMR analyses also indicated that there may be important changes in backbone dynamics, as evidenced by resonance broadening (*34*) and motion freezing (*32*, *33*) of the residues at the binding site. A detailed dynamics study of the KAPP-FHA domain has revealed a net increase in backbone rigidity upon phosphopeptide binding (*37*).

The mode of pThr recognition is highly conserved (Fig. 6A). To facilitate the comparison of key pThr-binding residues in different FHA domains, we have listed the residue number and the loop (for example, β3-β4 stands for the loop between the two strands) of these residues of some of the FHA domains in Table 1. The phosphate group is anchored through salt bridges, hydrogen bonds, or both, by conserved Arg (Arg^{70} in FHA1) and Ser (Ser^{85} in FHA1) residues and nonconserved residues, such as the one immediately following the Ser; for example, Asn^{86} in FHA1, Lys^{46} in Ki67 (antigen identified by monoclonal antibody K_i-67) (*38*), Arg^{48} in mouse PNK, and Arg^{61} in RNF8 (*11*, *14*, *32*, *34*) (Fig. 4A). In NMR studies, the amide proton of this conserved Ser residue in six different FHA domains—from Rad53 (FHA1 and 2), Chk2, Ki67, Dun1 (*39*), and nuclear inhibitor of protein phosphatase 1 (NIPP1) (*8*, *12*, *31*, *40*)—shows a characteristic downfield shift to around 11.5 to 12.5 parts per million upon binding of the pThr-peptide (Fig. 5C), in further support of microstructural similarity at the binding site. The methyl group of the pThr residue makes contacts with a number of FHA residues, for example, Ser^{82}, Arg^{83}, Thr^{106}, and Asn^{107} in FHA1 (*11*, *32*), which could explain how the FHA domain is prevented from binding to pSer residues.

The specificity toward the pThr+3 residue is not conserved (Table 2). Whereas Rad53-FHA1 displays a clear preference for an Asp residue because of the presence of Arg^{83} in the β4-β5 loop, Rad53-FHA2 preferentially binds to Ile or Leu, even though it appears to have an Arg (Arg^{617}) structurally equivalent to that of Rad53-FHA1. As revealed in the FHA2 structure, the latter is engaged in an intramolecular salt bridge with Asp^{683}, which makes its guanidino group unavailable for intermolecular recognition (*6*, *27*, *36*). In light of this structural information, the binding specificities of these two domains can be altered by rational site-directed mutagenesis (*41*), as we have illustrated (Fig. 6B).

Although the library approach and the structural determination of FHA domain complexes with short phosphopeptides derived from consensus motifs have provided valuable information in early studies of FHA domains, these methods have had their shortcomings. First, the practical

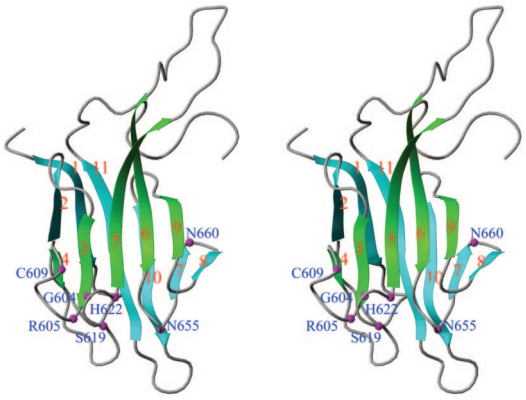

Fig. 3. Basic structural features of the FHA domain. Stereoview of the FHA2 domain of the *S. cerevisiae* kinase Rad53. The large β sheets are colored in green and blue, respectively, and the conserved residues highlighted in the sequence alignment are labeled. Note that in some studies the very short and parallel β4 strand was labeled as β3′ and the subsequent strands as β4-β10 instead of β5-β11.

number of random sites is five, or six at most (for example, XXXpTXXX, where X is a randomized amino acid), which limits the ability to test the roles of residues remote from the pThr site. Second, the selection of random residues may be biased toward highly charged peptides because the electrostatic term in the free energy calculations of protein-ligand recognition seems to contribute more to binding affinity (*42*, *43*). In addition, a large number of hydrophobic peptides may not dissolve in the binding buffer, thus reducing the number of possible candidate peptides that can be screened (*44*). Thus, many laboratories have actively pursued functional studies to identify binding partners and binding sites, and a wealth of insightful information has been generated.

Diversity of FHA-Ligand Interactions Based on Biological Approaches

Biological studies from many laboratories showed that the ligand specificity of FHA domains is much more diverse than that suggested by the so-called "pThr+3 rule" generalized from library screenings. It was found that, in addition to the pThrXX(Asp or Ile or Leu) specificity described above, there are three additional types of recognition specificities (Fig. 7).

FHA Domains with pThr+3 Specificities

FHA domains with specificities for pTXXD or pTXX(I/L/V). The pTXXD or pTXX(I/L/V) specificities (Fig. 7A) identified by library screening have been verified in a number of biological studies (Table 2). For instance, *S. cerevisiae* Rad53-FHA1 and the *Schizosaccharomyces pombe* checking DNA synthesis protein 1 (Cds1)–FHA domain both prefer a highly charged Asp residue at the pThr+3 position (*11*, *45*, *46*). On the other hand, FHA2 from S. cerevisiae Rad53 and FHA domains from human Chk2 and mediator of DNA-damage checkpoint–1 (MDC1) [also known as nuclear factor with an amino-terminal FHA domain and a tandem repeat of BRCT (breast cancer susceptibility gene–1 C-terminal) domains (NFBD1)] prefer a nonpolar residue at the pThr+3 position (Leu, Ile, or Val) (*11*, *18*, *47*, *48*). The PP2C-type phosphatases Ptc2 and Ptc3 are required in DNA checkpoint inactivation because of their interaction with Rad53, but only as a result of double-strand breaks induced by HO endonucleases (*49*). The interaction of Ptc2 or Ptc3 with Rad53 is mediated by the FHA1 domain (7-163) through a phosphorylation-dependent mechanism. Thr^{376} of Ptc2 (within a pTXXD motif) is the in vivo binding site for Rad53-FHA1 domain. Briefly, Ptc2 interacts with activated Rad53, dephosphorylates it, and consequently leads to cell cycle resumption and recovery after DNA damage (*45*).

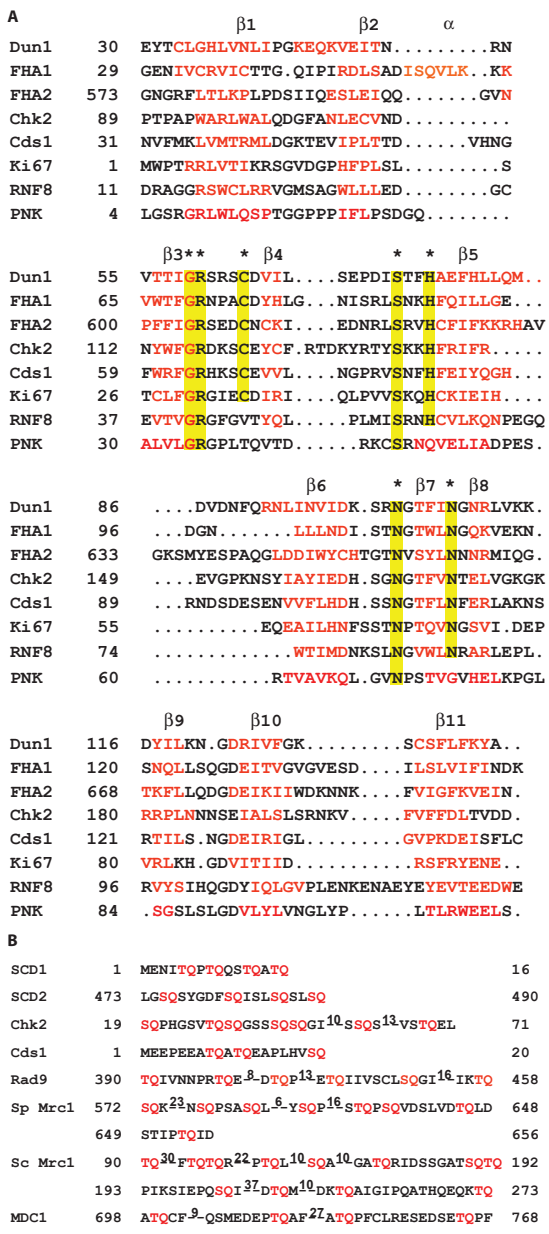

Fig. 4. Sequence alignments. (**A**) FHA domains. The residues colored in red highlight the 11 conserved β strands among FHA domains, while yellow highlights indicate conserved residues. Dun1, FHA1, and FHA2 are from *S. cerevisiae*, and Cds1 is from *S. pombe*. Chk2, RNF8, and Ki67 are human proteins. All FHA domain alignments are based on their structures except for that of Cds1-FHA, which is aligned on the basis of its sequence. (**B**) SCD domains. Proteins with SCD domains that have been discussed in this review are presented. There is no evident homology among these proteins, but SQ and TQ residues are highlighted in red to illustrate their proximity to each other in a short stretch of protein. The numbers of amino acid residues omitted are shown between the SQ-TQ repeats. Sc, *S. cerevisiae*; Sp, *S. pombe*.

Single FHA domain with multiple pThr+3 specificities. Biological studies identified modifier of damage tolerance–1 (Mdt1) as a binding partner of Rad53-FHA1, with Thr^{305} as the recognition site (*50*). However, the +3 residue from Thr^{305} is a hydrophobic Ile residue and not a charged Asp. How can the same FHA1 domain bind to two different phosphopeptides, one containing pTXXD and the other containing pTXXI? A detailed comparison of the binding interactions between FHA1 and the pTXXI peptide from Mdt1 with those of FHA1 and the pTXXD peptide from Rad9 (*51*) is shown in Fig. 8. The FHA1-pTXXI complex does indeed retain the features of FHA1-pTXXD in recognizing the pThr moiety, which is anchored by hydrogen bonding or salt bridges to Arg^{70}, Ser^{85}, Asn^{86}, and Thr^{106}. However, although the Asp in the FHA1-pTXXD complex is involved in a strong charge-charge interaction with the Arg^{83} of FHA1, the Ile of the FHA1-pTXXI complex may contribute substantially to the binding affinity by mediating hydrophobic interactions with Gly^{135} and particularly Val^{136}, which are located in the β10-β11 loop. Furthermore, residues other than pThr and the +3 residue also provide fine-tuning of the binding interactions between the FHA domain and its target peptide (*51*). In summary, structural data indicate that an FHA domain is able to bind to pTXXD and to pTXX(I/L/V) peptides by adapting to the different sequences of the phosphopeptide.

pThr+3 specificities identified from chemical versus biological approaches. An example of a discrepancy between chemical and biological approaches was observed in Rad9, a suggested binding partner of Rad53-FHA1, which contains five possible ThrXXAsp motifs. Phosphopeptides corresponding to these five sites were synthesized and tested for their binding affinities for Rad53-FHA1. The peptide with the lowest K_d was S^{188}LEV(pT)EADATFVQ^{200} (0.36 μM), which led to the suggestion that Thr^{192} of Rad9 was the likely binding site and the determination of the structure of the Rad9:Rad53-FHA1 complex (Fig. 8A) (*32*). However, in a subsequent report, the most favorable binding site of Rad53-FHA1 to Rad9 in vivo was shown to be Thr^{390}, which has a Val at the pThr+3 position (*48*). The discrepancy between the two approaches regarding the exact pThr site of Rad9 serves as one caution about the biological relevance of the chemical library approach. However, there are many other cases where chemical and biological approaches identified the same ligand specificity (*16*, *18*, *45*, *49*, *52*, *53*).

FHA Domains That Recognize Residues Both N-Terminal and C-Terminal to pThr

At least two FHA domains interact substantially with residues N-terminal to the pThr site (Fig. 7B). In murine PNK-FHA complexed with a peptide derived from its biological target XRCC4, only the residues N-terminal to pThr, cradled between the β2-β3 and β4-β5 loops, are essential for binding (*14*). This unusual binding behavior may be due to several basic residues in the FHA domain interacting with the acidic residues N-terminal to the pThr of the target protein (Fig. 9A). Analysis of a complex containing the FHA domain of *Mycobacterium tuberculosis* EmbR and a low-affinity phosphopeptide SLEV(pT)EADT (K_d = 185 μM) showed interactions similar to those observed in eukaryotic FHA-peptide complexes, with Asn^{348} interacting with Glu and Asp at positions pThr+1 and pThr+3, respectively. In addition, a nonconserved Leu residue in this bacterial FHA domain interacts with a Leu at the pThr-3 position of the peptide (*54*) (Fig. 9B). However, the biological relevance of these interactions remains to be validated because the phosphopeptide used in the structure was from *S. cerevisiae* Rad9 and not from the binding partner of EmbR in *M. tuberculosis*.

Dun1-FHA Contains Two pThr Sites

SCDs (SQ-TQ cluster domains) are abundant in various proteins, and there are two such domains in the Rad53 kinase of *S. cerevisiae*, which precede each of the two FHA domains. The Rad53-SCD1 domain consists of four Thr-Gln (TQ) sites at positions 5, 8, 12, and 15 (Fig. 4B) and is important for Rad53 dimerization and activation (*55*, *56*). Furthermore, Stern and coworkers demonstrated that the Dun1-FHA domain interacts with the phosphorylated SCD1 of Rad53, which leads to activation of Dun1 (*56*). It is an intriguing question how such a phosphorylation cluster orchestrates the sequential activation of two separate kinases in a temporally ordered manner. Our own study indicates that Rad53-FHA1 recognizes singly phosphorylated SCD1, whereas Dun1-FHA specifically binds to SCD1 with dual phosphorylation at Thr^5 and Thr^8 (Fig. 9, C and D) (*33*). The structure of the dual pThr complex indicates that the first pThr-binding site is formed mainly by the conserved Arg^{60} residue and assisted by a nonconserved Arg^{62} located in the β3-β4 loop and that the second pThr-binding site consists of the mostly nonconserved Arg^{102} residue with possible assistance from Lys^{100} located in the β6-β7 loop. In addition, Ser^{11} at the +6 position relative to the first pThr also makes a considerable contribution to the binding, as evidenced by strong nuclear Overhauser effects (NOE) between this residue and Lys^{129} of Dun1-FHA in the β10-β11 loop. In vivo studies also showed that phosphorylation of both Thr^5 and Thr^8 on SCD1 is required for Dun1 to be fully activated and for the Dun1-dependent transcriptional DNA damage response, whereas single phosphorylation was sufficient for Rad53 to be fully activated and for Rad53-dependent cell survival. The existence of double phosphorylation of Thr^5 and Thr^8 and its enhancement upon DNA damage were further corroborated by mass spectrometry analyses (*33*).

The recognition of dual pThr residues by Dun1-FHA (Fig. 7C) is unprecedented among FHA domains. The results also shed light on the biological functions of the cluster of phosphorylation sites, suggesting a potential mechanism of sequential phosphorylation to direct a cascade of signaling events. Database searches have indicated that some other FHA domains could also possess dual pThr-recognizing specificities (*33*).

Ki67-FHA Recognizes an Extended Binding Surface

The Ki67 antigen protein, which contains 3256 amino acid residues, includes an FHA domain near its N terminus. Ki67 is widely used as an indicator of growth in cell populations because of its absence in resting cells (cells in G_0 phase) and its readily detectable nuclear localization and association with condensed chromosomes during interphase and mitosis, respectively (*57*). The biological function of Ki67, however, is little known. In addition to its suggested role in cell cycle progression, its involvement in the organization of higher-order chromatin structures has also been postulated (*58*). Through yeast two-hybrid screening, Yoneda's group identified human kinesin–like protein 2 (Hklp2) and human nucleolar protein interacting with the FHA domain of pKi67 (hNIFK) as the binding partners of the Ki67-FHA domain (*59*, *60*) and proposed that Hklp2 is likely phosphorylated during the mitotic phase, during which its interaction with Ki67-FHA is at its strongest.

After unsuccessful attempts to identify short phosphopeptides that bind to Ki67-FHA, we showed that the synthetic fragment consisting of residues 226 to 269 of hNIFK binds tightly to Ki67, provided that Thr^{234} is phosphorylated. In vitro kinase assays showed that Thr^{234} is phosphorylated by glycogen synthase kinase 3 (GSK3), but only if Thr^{238} is first phosphorylated by cyclin-dependent kinase 1 (CDK1)–cyclin B (*34*, *40*, *61*). The structure of the Ki67-FHA complex with hNIFK (226-269) phosphorylated at Ser^{230}, Thr^{234}, and Thr^{238} was then solved by NMR spectroscopy, which showed an extended binding surface for protein-phosphoprotein interactions (Fig. 7D). A particularly interesting feature is that the β strand of the peptide stacks with the β sheet of Ki67-FHA (Fig. 10). In addition, the interaction of a large number of hydrophobic residues with the peptide was also considerably different from what was observed with other FHA domain complexes (*61*). This structure represents the most extensive structural information of a complex between an FHA domain and a phosphoprotein and clearly shows that the interaction goes beyond the short stretch surrounding the pThr site. This structure also provides a basis for the quantitative evaluation of specific interactions. For example, changing $pThr^{234}$ to $pSer^{234}$ led to a decrease in the binding

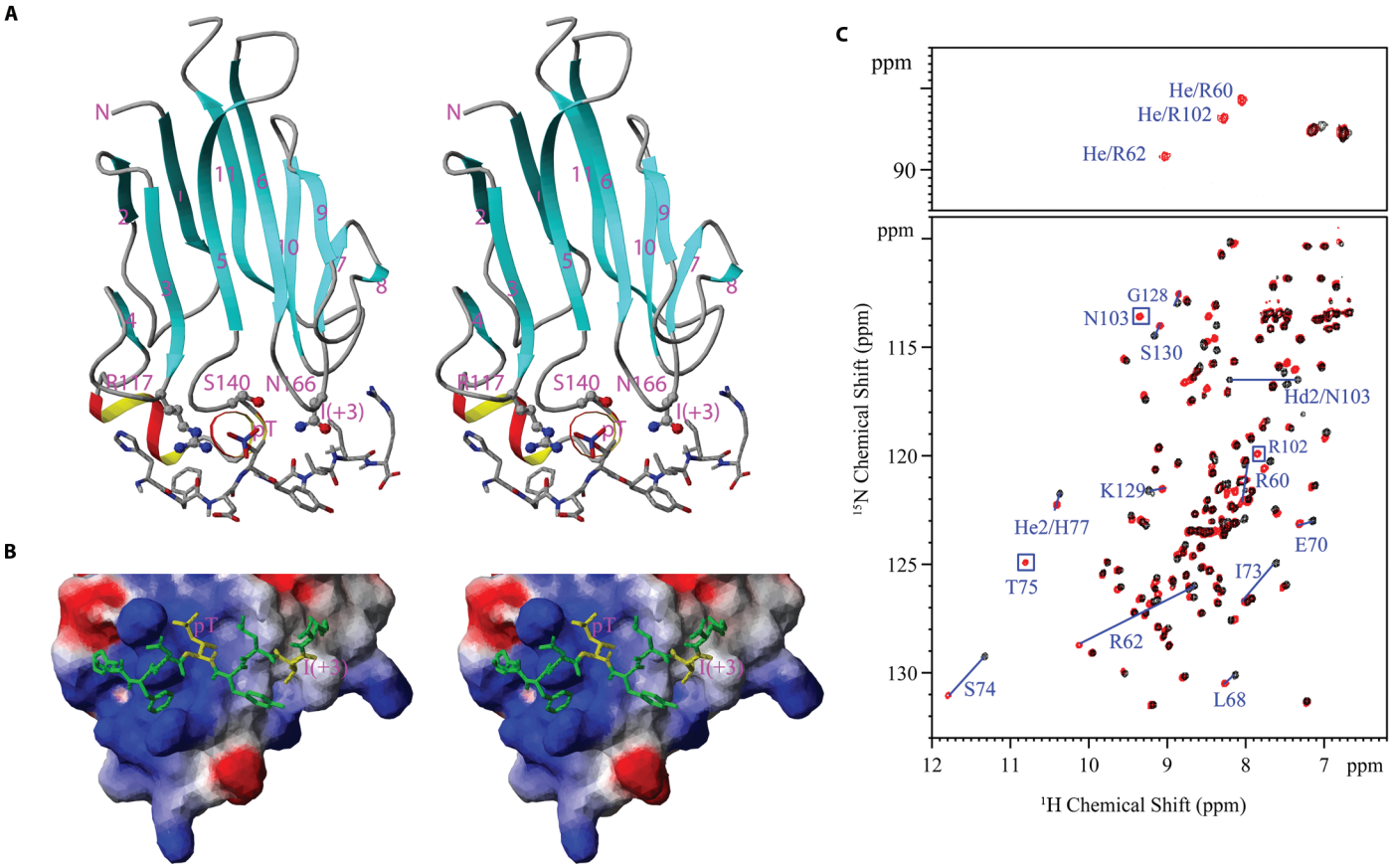

Fig. 5. FHA-phosphopeptide complexes. (**A**) Crystal structure of the complex formed between Chk2-FHA and a pThr peptide [RHFD(pT)YLIRR] [Protein DataBank (PDB) ID: 1GXC] (*13*). The side chains (heavy atoms only) of three conserved FHA domain residues are shown in ball-and-stick representation, whereas the peptide residues (heavy atoms only) are in stick representation. The carbon, nitrogen, oxygen, and phosphorus atoms are shown in gray, cyan, red, and blue, respectively. (**B**) Surface charge distribution of the same complex. Positive, negative, and neutral potentials are represented in blue, red, and white, respectively. The peptide residues pThr and Ile (pThr+3) are highlighted in yellow; the remainder are in green. (**C**) Two-dimensional ^{1}H-^{15}N HSQC NMR spectra of Dun1-FHA in free (black) and complex (red) forms. The peptide is the doubly phosphorylated Rad53 SCD1 peptide ^{3}NI(pT)QP(pT)QQST^{12}. Several important residues that exhibit large chemical shift perturbations (for example, Arg^{62}, Ser^{74}, Lys^{129}, and Ser^{130}) or reappear in the complex form [Thr^{75}, Arg^{102}, and Asn^{103} (boxed)] are labeled. The top panel shows the changes in NH$^{\varepsilon}$ of Arg.

affinity of Ki67-FHA for hNIFK (226-269) by a factor of 70 (K_d increased from 0.077 to 5.5 μM), whereas deleting the β strand from the peptide led to a decrease in the binding affinity by a factor of 180. On the other hand, individual substitutions of the –1, +1, +2, and +3 residues with Ala resulted in very small effects on binding affinity (a factor of <4), which is a clear indication that the "pThr+3 rule" does not apply to the Ki67-FHA domain. The residues surrounding pThr appear to regulate the phosphorylation of Thr^{234} by GSK3 (*34*).

FHA Domains Mostly Use Loops for Ligand Binding and Specificity Control

It is beyond the scope of this review to make detailed comparisons between FHA domains and other protein-protein interaction domains. However, a cursory comparison of the FHA domain with three well-studied domains, 14-3-3 (specific for pSer and pThr) (*62*), SH2 (specific for pTyr) (*63*), and WW (specific for proline-rich sequences, or pThr-pSer containing trans-proline) (*64*) (Fig. 11), indicates that the FHA domain is unique in that its binding site mostly involves its loops. It is important to note that in addition to the β3-β4, β4-β5, and β6-β7 loops observed in early structural studies with synthetic peptides (*11*, *13*, *32*, *36*), the involvement of the β10-β11 loop in pThr-peptide binding was clearly observed in later structural studies of Rad53-FHA1, Ki67-FHA, and Dun1-FHA complexed with their physiologically relevant targets. Briefly, intermolecular NOE assignments showed that Val^{136} in Rad53-FHA1 (*51*), Ile^{91} in Ki67-FHA (*34*), and Lys^{129} in Dun1-FHA (*33*) interacted with peptide residues C-terminal to the pThr. Furthermore, it was also suggested, on the basis of peptide-induced chemical shift perturbation experiments, that the β8-β9 loop of the FHA domain of kinase-associated protein phosphatase (KAPP), which apparently is the longest among the structurally determined FHA domains, could be involved in binding (*10*). Thus, because the loops and turns connecting β strands are typically flexible in conformation, variable in length, and divergent in sequence, particularly those (for example, the β10-β11 loop) beyond the core FHA homology region, this might explain the diverse ligand-binding specificities exhibited by various FHA

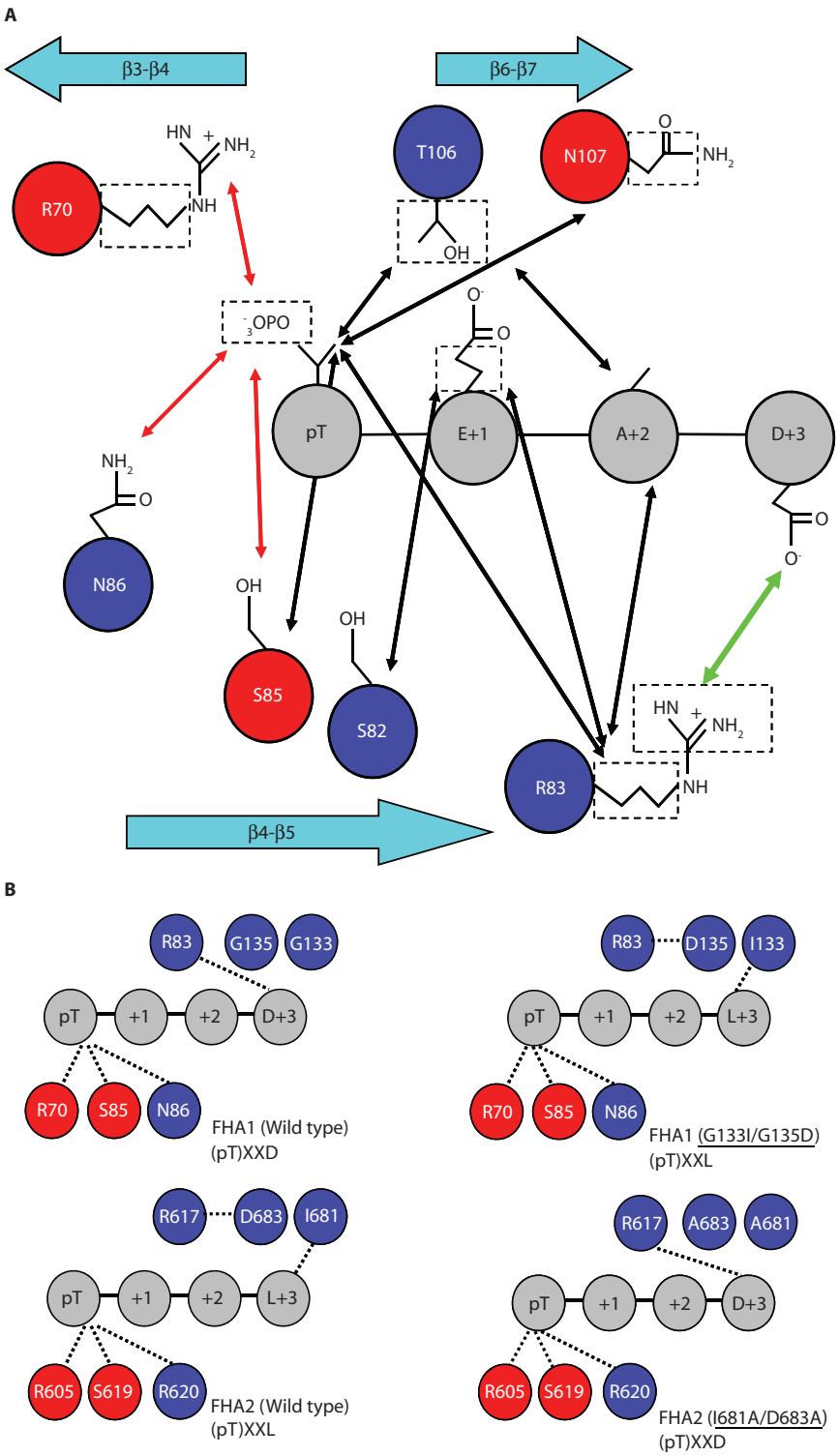

Fig. 6. Schematic representation of the structural basis of the pTXXD specificity of FHA1 for pTXXD compared with the specificity of FHA2 for pTXXL. (**A**) Illustration of the specificity of Thr versus Ser (highlighted by a number of interactions between pThr-γCH_3 and the protein). Other interactions, demonstrated by intermolecular NOEs observed between conserved residues, nonconserved residues, or both, of the Rad53-FHA1 domain and the pThr peptide from Rad9, are also presented (*32*). The ionic interactions involving phosphate group, hydrophobic interactions, and the electrostatic interactions involving Arg^{83} are indicated in red, black, and green, respectively. (**B**) Illustration of specificity at the pThr and pThr+3 positions. Conserved and nonconserved residues among the two domains are highlighted in red and blue, respectively (*41*).

domains, which in turn provides structural and functional versatility to FHA domain–containing proteins.

Biological Functions of FHA Domains

The diverse biological functions of FHA domains are highlighted in Fig. 2. Here, we briefly review several FHA domain–containing proteins. Because it is not possible to cover all the published literature, we place more emphasis on the systems that have also been studied for their structures and ligand specificities.

Checkpoint Signaling in Humans: Chk2, RNF8, NBS1, and MDC1

Chk2. Human Chk2 consists of an SCD and an FHA domain N-terminal to the kinase domain (Fig. 1B). Chk2, together with Chk1, plays a critical role in cell cycle regulation, DNA repair, and DNA damage–induced apoptosis at G_1/S, S, and G_2/M checkpoints (*65*) (Fig. 2). Chk2 relays the DNA damage signal from the serine-threonine kinases ATM (ataxia telangiectasia, mutated) or ATR (ATM and Rad3-related), which phosphorylate Chk2 at Thr^{68} in its SCD (*66*). Consequently, the Chk2-FHA domain binds to the $pThr^{68}$ of a second Chk2 molecule, which leads to dimerization, oligomerization, or both of Chk2, followed by autophosphorylation at the kinase activation loop for complete activation of Chk2 (*16*, *18*) (Fig. 12A). Activated Chk2 phosphorylates and interacts with its downstream effectors, which leads to either halted cell cycle progression to provide time to enable repair of DNA, or the triggering of apoptosis if damage cannot be repaired (*65*) (Fig. 2). Another upstream mediator, E3 identified by differential display (EDD), which is a human homolog of *Drosophila melanogaster* "hyperplastic discs" and functions as an E3 ubiquitin ligase, associates with Chk2 through its FHA domain. Knockdown of EDD by small interfering RNA (siRNA) inhibited DNA damage–dependent phosphorylation of Thr^{68}, thus making Chk2 incapable of responding to DNA damage (67). Breast cancer susceptibility gene–1

(BRCA1), a substrate of Chk2, interacts with Chk2 through phosphorylation-dependent binding with its FHA domain (*13*).

Chk2 is a tumor suppressor; mutations in the *Chk2* gene were identified in a subset family of malignancy-prone Li-Fraumeni syndromes and in sporadic human cancers (*68*). The Chk2-FHA functions as both a phosphorylation-dependent and -independent mediator to link upstream activators with downstream targets, according to studies of the oncogenic mutations ($Arg^{117} \rightarrow Gly^{117}$, $Arg^{145} \rightarrow Trp^{145}$, and $Ile^{157} \rightarrow Thr^{157}$) within the FHA domain (*13*, *16*, *18*, *69*). The $Arg^{117} \rightarrow Gly^{117}$ mutation occurs in the conserved region for pThr-binding and attenuates the autokinase activity in response to DNA damage (*69*). The locations of the other two oncogenic mutations, $Arg^{145} \rightarrow Trp^{145}$ and $Ile^{157} \rightarrow Thr^{157}$, are remote from the binding pocket of pThr. It is interesting that the $Arg^{145} \rightarrow Trp^{145}$ mutant cannot bind to the original pThr ligand. Arg^{145} is located in the core structure (β5) of FHA β strands, and the $Arg^{145} \rightarrow Trp^{145}$ mutation destabilizes Chk2 and prevents the transphosphorylation activity of ATM (*18*, *70*, *71*). On the other hand, the $Ile^{157} \rightarrow Thr^{157}$ mutant behaves like the wild-type (WT) protein in terms of Chk2 activation; however, this mutant fails to bind to the downstream target of ectopically expressed BRCA1, p53, and cell division cycle 25A (CDC25A) (*13*, *72*, *73*).

RNF8. A recent addition to the family of checkpoint regulators is RNF8 (Fig. 1A), a novel DNA damage–response protein that is recruited to the chromatin that flanks DNA lesions, where it colocalizes with phosphorylated H2AX, a variant of histone H2A, phosphorylated ATM, MDC1, BRCA1, 53BP1, RAP80, and NBS1 (*30*, *74–76*) (Fig. 12B). These interactions lead to the formation of ionizing radiation (IR)–induced foci (IRIF) in response to DNA double-strand breaks (*30*, *74–76*). Knockdown of RNF8 by siRNA prevents adequate cell cycle arrest at the G_2/M checkpoint when IR is applied (*30*). RNF8 acts downstream of γH2AX (phosphorylated H2AX) and MDC1; the targeting of RNF8 to DNA lesions is facilitated by MDC1 through its phosphorylation-dependent interaction with the RNF8-FHA domain (*30*, *75*, *76*). Assembly of other downstream checkpoint proteins, such as BRCA1, 53BP1, and RAP80, at the IRIF requires RNF8 to ubiquitinate the histones flanking the site of the DNA lesion (*30*, *74–76*) (Fig. 12B). The RNF8-FHA domain shows a high specificity for Tyr and Phe at the pThr+3 position, as determined by the aforementioned library screening, and the structure of the complex it forms with phosphopeptide has been solved by x-ray crystallography (*30*). The RNF8-FHA–oriented motifs of pTXX(F/Y) can be narrowed down to the four-TQ cluster–containing sequence of MDC1 from residues 698 to 768; the consensus sequence for the four binding sites is TQXF, which is phosphorylated by ATM (*30*, *76*). K_d values for the binding of the four synthetic phosphopeptides encompassing the binding regions of MDC1 to the RNF8-FHA domain are in the range of 3 to 11 μM (*30*). Deletion of this putative RNF8-FHA domain–binding region (residues 698 to 768) of MDC1 abolishes its interaction with RNF8 and prevents the assembly of downstream checkpoint proteins at sites of DNA lesions (*30*). Thus, the FHA domain is required for RNF8 functions in orchestrating the DNA damage response for the assembly of checkpoint proteins and signal transduction at the sites of DNA damage (*30*, *75*, *76*).

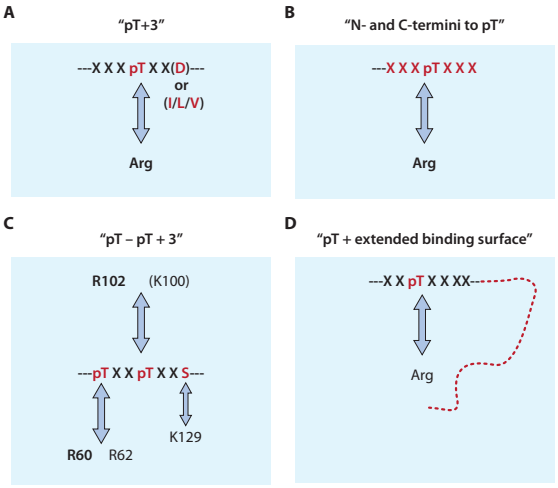

Fig. 7. Illustration of four different mechanisms of ligand binding by FHA domains. (**A**) Schematic illustration of the "pThr+3" mechanism, in which some FHA domains recognize their targets mainly by the presence of the pThr and the residue at the +3 position (*11–13*, *36*). (**B**) The "N- and C-termini to pThr" mechanism of FHA domain interaction involves amino acid residues both N-terminal and C-terminal to the pThr residue (*14*). (**C**) The "pThr-pThr+3" mechanism was recently discovered for the yeast Dun1-FHA domain. Recognition specificity was determined by two pThr residues and the +3 position of the second pThr (*33*). (**D**) The "pThr + an extended binding surface" mechanism is required for the interaction between the Ki67-FHA domain and its binding partner NIFK (*34*).

NBS1 and MDC1. NBS1 and MDC1 (also known as NFBD1) are two other important checkpoint signaling proteins, both of which contain FHA and BRCT domains (Fig. 1A). NBS1 was first identified from a protein mutated in Nijmegen breakage syndrome, which is characterized by chromosome instability, radiosensitivity, and a high frequency of malignancies (*77*, *78*). NBS1 also forms a complex with meiotic recombination 11 (MRE11) and RAD50, which presumably functions in sensing DNA double-strand breaks (DSBs) in the DNA damage–response pathway, as well as tethering and editing two DNA ends in the homologous recombination repair pathway (*79*) (Fig. 12B).

NBS1 is not only a downstream target of ATM, but also acts upstream to promote optimal ATM activation and its recruitment to the flanking region of DSBs (*80*, *81*). The unwinding of DNA ends by the MRE11:RAD50:NBS1 (MRN) complex is essential for stimulating the monomerization and activation of ATM (*82*). Activated ATM then phosphorylates H2AX at Ser^{139} neighboring the DNA lesion that serves as a docking site (*83*), which in turn attracts the BRCT repeat of MDC1 through its pSer-binding activity (Fig. 12B) (*84*). Meanwhile, the consecutive SDTD (Ser-Asp-Thr-Asp) motifs of MDC1, when phosphorylated by casein kinase 2 (CK2), are bound by the FHA domain (*85*, *86*) and the adjacent BRCT repeat (*87*, *88*) of NBS1; such binding directs the accumulation of the MRN complex to damaged chromatin. Furthermore, the recruited MDC1 acts as a molecular scaffold by accommodating additional ATM molecules through interactions of its FHA domain with phosphorylated ATM (*89*). This therefore provides an important feedback loop that amplifies ATM-dependent γH2AX signals at sites of damage by which MDC1 may promote downstream effector proteins that accumulate after the induction of DSBs (*89*). Alternatively, the FHA domain of MDC1 also interacts directly with $pThr^{68}$ of Chk2 (*47*) and with MRE11 (*90*),

whereas knockdown of MDC1 by siRNA attenuates the phosphorylation of p53 at Ser^{20} by Chk2 and decreases IR-induced p53 stabilization, which results in a weakened apoptotic response (*47*). The knockdown also abates IRIF formation of the MRN complex, 53BP1, BRCA1, and γH2AX (*91*), which is suggestive of fundamental roles for MDC1 in mediating DNA-damage checkpoints.

PNK and ATPX in the Regulation of DNA Repair Pathways

In addition to DNA-damage signaling mediated by NBS1 and/or MDC1, which presumably facilitates or is essential for the repair of DNA DSBs by homologous recombination (*92*–*94*), the FHA domain is also involved in other DNA-repair mechanisms. Mammalian PNK has DNA-kinase and DNA-phosphatase activities and is responsible for maintaining 5′-phosphate and 3′-hydroxyl termini at DNA-strand breaks, a prerequisite for polymerases and ligases operating in DNA repair (*95*). PNK is recruited to sites of base excision repair (BER) and nonhomologous end-joining (NHEJ) repair through its N-terminal FHA domain interacting with CK2-phosphorylated pThr residues of XRCC1 and XRCC4 (x-ray repair complementing defective repair in Chinese hamster cells 1 and 4, respectively), two key components of BER and NHEJ repair pathways that complex with DNA ligases III and IV, respectively (*96*, *97*). In support of this, a crystallographical study of PNK shows that its FHA domain binds to an XRCC4-derived phosphopeptide (*14*); more specifically, it exhibits the highest selectivity for residues N-terminal of pThr, some selectivity for C-terminal residues, and no selectivity for the pThr+3 position (Fig. 9A) (*96*).

The FHA domain of aprataxin (APTX), a protein also involved in DNA repair and genomic stress (*98*), contains the same conserved residues involved in phosphopeptide recognition as does the PNK-FHA (*14*), which may suggest that the same ligand-sequence selectivity is shared between these two FHA domains. Indeed, APTX also forms complexes in vivo with XRCC1/ligase III and XRCC4/ligase IV and has been proposed to facilitate PNK activity during BER and NHEJ repair mechanisms (*99*, *100*). Nevertheless, in contrast to the PNK-FHA, the APTX-FHA shows high specificity for a triply phosphorylated peptide derived from XRCC1 with a charged residue at the pThr+3 position (*99*).

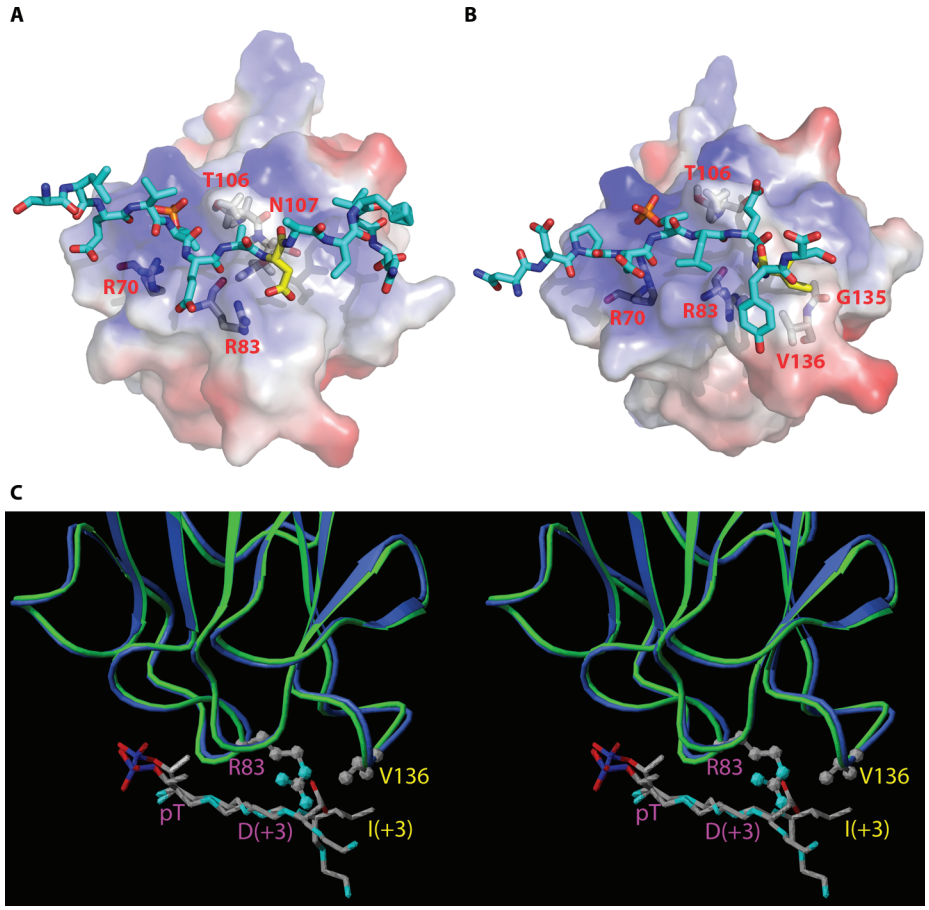

Fig. 8. Comparison of structures of FHA1 in complex with pTXXI and pTXXD phosphopeptides. (**A**) Surface-charge diagram of Rad53-FHA1 with a pThr peptide (SLEVpT^{192}EADATFVQ) from Rad9 (PDB ID: 1J4Q) (*32*). (**B**) Surface-charge diagram of Rad53-FHA1 with a pThr peptide (NDPDpT^{305}LEIYS) from Mdt1 (PDB ID: 2A0T) (*51*). (**C**) Stereoview showing the overlay of FHA1 structures in complex with pTXXI (PDB code 2A0T) and pTXXD (PDB code 1K3Q) phosphopeptides. The FHA1 domain is shown in a ribbon diagram colored in blue (FHA1-pTXXI complex) and green (FHA1-pTXXD complex). Several residues are highlighted: Val^{136} in FHA1-pTXXI, Arg^{83} in FHA1-pTXXD, and the peptide pThr and pThr+3 residues. The atoms are colored as for Fig. 5A. It appears that the pThr moiety is recognized in essentially the same way for both complexes. However, although there is strong ionic interaction between Asp(pT+3) and Arg^{83} in FHA1-pTXXD, the Ile(pThr+3) in FHA1-pTXXI contributes substantially to the binding through a hydrophobic interaction with the Val^{136} of FHA1 and so moves the residues C-terminal to pThr from the β6-β7 loop to the Val^{136}-residing β10-β11 loop.

Taken together, these two FHA domains are likely to use different phosphopeptide-binding specificities to interact with the same binding partners in order to regulate each other's activities. Recently, PALF [PNK and APTX-like FHA protein, also known as APLF (aprataxin and PNK-like factor)] was identified by two laboratories and shown to contain an FHA domain and a zinc finger–like CYR (Cys-Tyr-Arg) motif. This protein directly interacts with Ku86, ligase IV, and phosphorylated XRCC4 proteins; has endonuclease and exonuclease activities; and thus plays roles similar to this category of proteins in DNA damage (*101*, *102*). The binding specificities of its FHA domain have not yet been determined.

Cds1, Rad53, and Dun1 in Checkpoint Signaling in Yeast

Here, we discuss Chk2 homologs in yeast: Cds1 in *S. pombe* and Rad53 and Dun1 in *S. cerevisiae*. The domain structures of these three yeast kinases are similar, but not identical, to Chk2 (Fig. 1B). Dun1 lacks an SCD preceding its FHA domain,

Species	Protein	Residues	Method	Phosphopeptide	Source of peptide	Key FHA residues for canonical pT binding	PDB code	Ref.
S. cerevisiae	Rad53	573–730 (FHA2)	NMR				1QU5	(*8*)
S. cerevisiae	Rad53	573–730 (FHA2)	NMR	EDI(pY)YLD†	826–832 Rad9		1FHR	(*27*)
S. cerevisiae	Rad53	573–730 (FHA2)	NMR	EVEL(pT)QELP†	599–607 Rad9	R605 (β3-β4), S619, R620 (β4-β5), T654 (β6-β7)	1K2N	(*36*)
S. cerevisiae	Rad53	2–164 (FHA1)	NMR				1G3G	(*12*)
S. cerevisiae	Rad53	14–164 (FHA1)	X-ray	SLEV(pT) EADATFAKK†	188–198 Rad9	R70 (β3-β4), S85, N86 (β4-β5) T106 (β6-β7)	1G6G	(*11*)
S. cerevisiae	Rad53	14–164 (FHA1)	NMR	SLEV(pT) EADATFVQ†	188–200 Rad9	Same as 1G6G	1K3Q	(*32*)
S. cerevisiae	Rad53	14–164 (FHA1)	NMR	KKMTFQ(pT) PTDPLE†	148–160 Rad9	Same as 1G6G	1K3N	(*32*)
S. cerevisiae	Rad53	14–164 (FHA1)	NMR	NDPD(pT)LEIYS*	301–310 Mdt1	Same as 1G6G	2A0T	(*51*)
S. cerevisiae	Rad53	14–164 (FHA1)	NMR	NI(pT)QPTQQST*	3–12 Rad53	Same as 1G6G	2JQI	(*33*)
S. cerevisiae	Dun1	19–159	NMR				2JQJ	(*33*)
S. cerevisiae	Dun1	19–159	NMR	NI(pT)QP(pT) QQST*	3–12 Rad53	R60, R62 (β3-β4)	2JQL	(*33*)
M. tuberculosis	EmbR	285–382	X-ray				2FEZ	(*54*)
M. tuberculosis	EmbR	285–382	X-ray	SLEV(pT)EADT†	188–197 Rad9	R312 (β3-β4) S326, R327 (β4-β5), S347 (β6-β7)	2FF4	(*54*)
A. thaliana	KAPP	180–313	NMR				1MZK	(*10*)
A. thaliana	Y4449	1–105	NMR				1UHT	
M. musculus	PNK	1–106	NMR				1UJX	
M. musculus	PNK	1–110	X-ray	YDES(pT) DEESEKK*	229–240 XRCC4	R35 (β3-β4), S47, R48 (β4-β5)	1YJM	(*14*)
M. musculus	NIPP1	1–132	NMR				2JPE	(*35*)
M. musculus	AFAD	381–487	NMR				1WLN	
H. sapiens	Chk2	92–207	X-ray	RHFD(pT)YLIRR†	Synthetic	R117 (β3-β4), S140, K141 (β4-β5)	1GXC	(*13*)
H. sapiens	CHFR	14–128	X-ray				1LGQ	(*15*)
H. sapiens	CHFR	14–128	X-ray	Tungstate			1LGP	(*15*)
H. sapiens	Ki67	1–120	NMR				1R21	(*40*)
H. sapiens	Ki67	1–120	NMR	KTVD(pS) QGP(pT)PVC(pT) PTFLERRKSQ VAELNDDDKDD EIVFKQPISC*	226–269 hNIFK	R31 (β3-β4), S45, K46 (β4-β5) T66 (β6-β7)	2AFF	(*34*)
H. sapiens	PNK	8–108	X-ray				2BRF	
H. sapiens	RNF8	8–139	NMR				2CSW	
H. sapiens	RNF8	13–146	X-ray	ELKpTERY	Synthetic	R42 (β3-β4), S60, R61 (β4-β5)	2PIE	(*30*)
H. sapiens	KIF1C	498–599	X-ray				2G1L	
H. sapiens	KIF1B	531–647	NMR				2EH0	

*From biological studies. †From peptide library screening.

Table 1. Structures of free FHA and FHA domain–phosphopeptide complexes. Conserved residues are underlined.

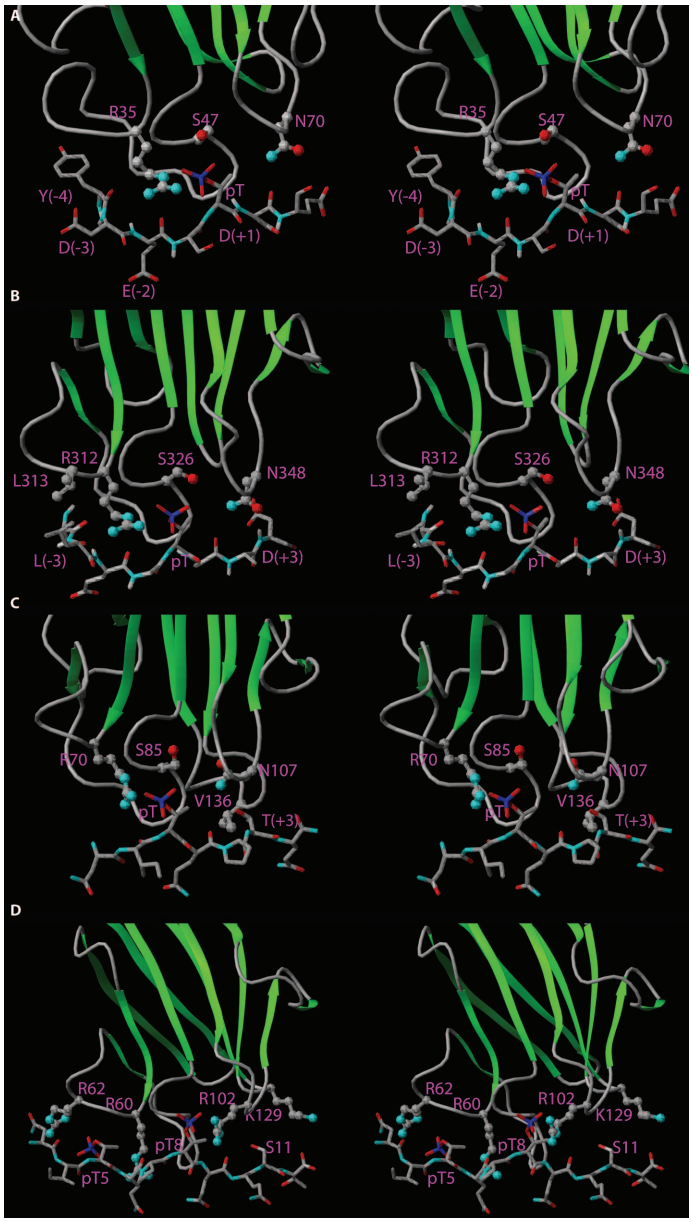

Fig. 9. Stereoview of structures of FHA domain complexes with phosphopeptide fragments derived from biological studies. (**A**) The binding of PNK-FHA to a pThr peptide YDES(pT)DEESEKK from XRCC4 (PDB ID: 1YJM) (*14*). (**B**) The binding of EmBR-FHA with a synthetic pThr peptide SLEV(pT)EADT (PDB ID: 2FF4) (*54*). (**C**) Structure of Rad53-FHA1 in complex with a singly phosphorylated Rad53-SCD1 peptide ^{3}NI(pT)QPTQQST^{12} (PDB ID: 2JQI). (**D**) Structure of Dun1-FHA in complex with a doubly phosphorylated Rad53 SCD1 peptide ^{3}NI(pT)QP(pT)QQST^{12} (PDB ID: 2JQL). Several important FHA residues are shown in ball-and-stick representation (heavy atoms and side chains only), whereas the peptide residues (heavy atoms only) are in stick representation. The atoms are colored similarly to those in Fig. 5A.

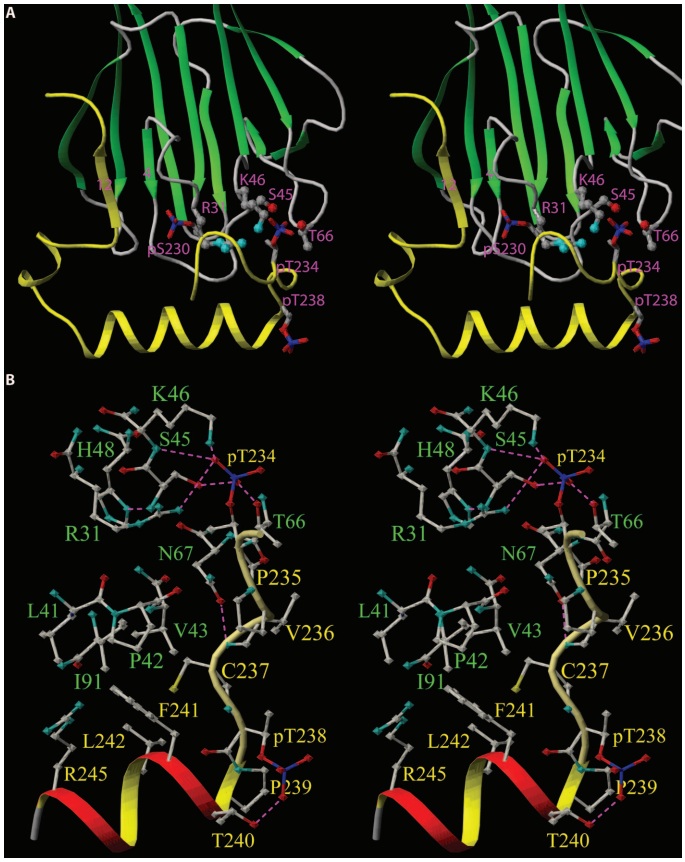

Fig. 10. Stereoview of the Ki67-FHA:NIFK (226-269)3P complex (*34*). (**A**) The ribbon diagram shows overall interactions. Four FHA residues important for pThr^{234} binding together with the three phosphorylated residues are highlighted, and the two β strands engaged in intermolecular β sheets are numbered (PDB ID: 2AFF). (**B**) Detailed interactions in this complex involving pThr^{234} and the +1, +2, and +3 residues of hNIFK and the interface between the binding loops of Ki67-FHA and the α helix of hNIFK are shown. Carbon, nitrogen, oxygen, sulfur, and phosphorus atoms are colored in gray, cyan, red, yellow, and blue, respectively. Some of the predicted hydrogen bonds are depicted with dashed lines.

whereas Rad53 contains two sets of SCD-FHA domains. The discussion below will focus on the roles played by the FHA domain in the activation of these kinases in response to DNA-damage or replication stress. As described above, Chk2 is activated by a two-stage process: FHA-independent phosphorylation by an upstream kinase, followed by FHA-dependent dimerization and autophosphorylation. The three yeast kinases largely follow the same two-stage processes; however, the molecular mechanisms mediated by their FHA domains vary substantially in each case (Fig. 12A).

Cds1. In *S. pombe* Cds1, the FHA domain is involved in both phosphorylation of Cds1 by upstream kinases and autophosphorylation of Cds1 (*46*). Phosphorylation of Cds1 is mediated by the TQ repeats (Thr^{645} to Gln^{646} and Thr^{653} to Gln^{654}, Fig. 4B) of mediator of replication checkpoint protein 1 (Mrc1) (*46*, *103*). Upon replication stress, Cds1-FHA binds to pThr^{645} and pThr^{653} of Mrc1, which leads to the recruitment of Cds1 to the upstream kinase Rad3,

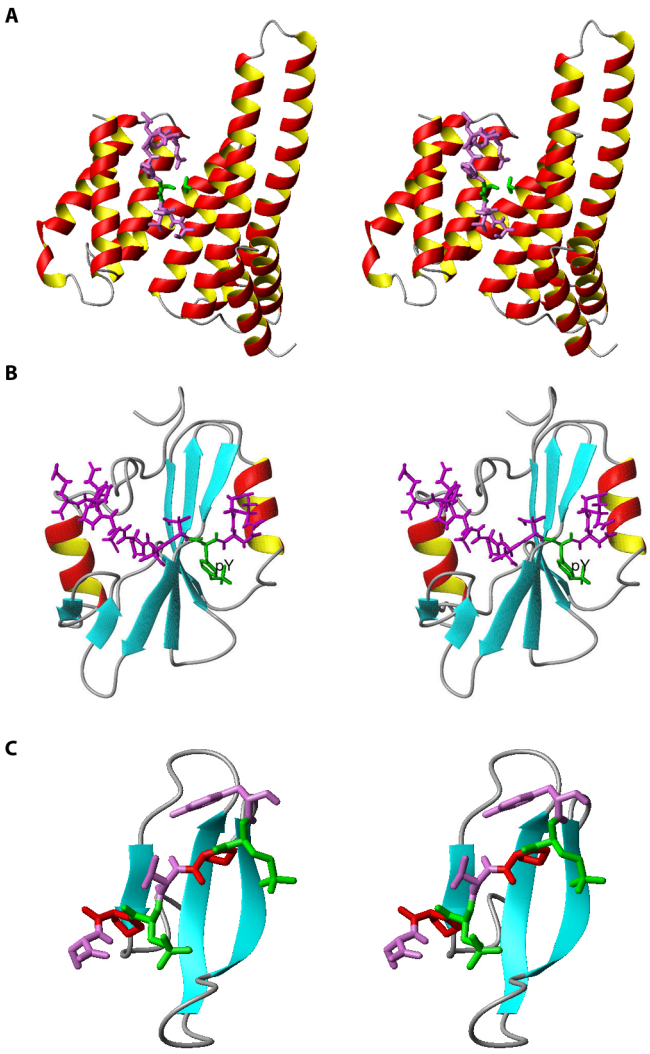

Fig. 11. Stereoviews of structures of other protein-protein interaction domains. (**A**) X-ray structure of the 14-3-3 domain in complex with a phosphopeptide RLYH(pS)LPA (PDB code: 1QJA) (*134*). (**B**) Solution structure of the C-terminal SH2 domain of PLC-γ1 in complex with a phosphopeptide DND(pY^{1021})IPLPDPK from the PDGF receptor (PDB code: 2PLD) (*135*). (**C**) X-ray structure of the pin1 WW domain with doubly phosphorylated serines followed by prolines T(pS)PT(pS)PS (although only the second pSer is involved in binding) from the C-terminal domain of RNA polymerase II (PDB code: 1F8A) (*136*). Phosphorylated residues (Tyr, Ser, or Thr) are shown in green, prolines in red, and the remainder of the peptide in purple.

which subsequently phosphorylates Thr^{11} of the Cds1-SCD (*52*, *53*). The Cds1-FHA domain then binds to pThr^{11} of the Cds1-SCD, which leads to dimerization and autophosphorylation of Cds1 (*46*) (Fig. 12A). Note that both TQ repeats of Mrc1 share the consensus sequence surrounding pThr (Fig. 4B) and redundantly interact with Cds1-FHA to activate Cds1. Furthermore, the Asp residue in the pThr+3 position matches that identified in the phosphopeptide motif pTXXD in vitro, and mutation of both Asp residues to Ala (Asp^{648} → Ala^{648} and Asp^{658} → Ala^{658}) results in hydroxyurea sensitivity (*46*). The K_d values of synthetic peptides encompassing pThr^{11} within Cds1-SCD and pThr^{653} within Mrc1-SCD for the Cds1-FHA domain are approximately 3.8 and 0.27 μM, respectively (*46*). In addition, Cds1 inhibits the activity of Mus81, a structure-specific endonuclease that plays a role in recombination, through its FHA domain. Thus, Cds1-FHA helps to maintain genomic integrity during certain types of replication stress (*104*).

Rad53. Checkpoint responses of *S. cerevisiae* Rad53 are required for DNA damage–induced signaling and for cell cycle arrest. They are invoked in the event of DNA damage that occurs at various stages of the cell cycle (G_1/S, S-phase progression, and G_2/M transitions) or inhibition of DNA replication (*105*–*107*). Rad53 is also essential for cell viability (*108*), normal cell growth, and transcriptional regulation (*109*). The mechanism of transactivation of Rad53 may be analogous to that of *S. pombe* Cds1 but could be substantially more complicated (Fig. 12A).

Rad53 has two FHA domains, FHA1 (*12*) and FHA2 (*8*), which have become prototypical of studies of the structure-function relationship of the FHA domain since the landmark work by Stern's group (*24*). These FHA domains may play diverse and overlapping roles in regulating Rad53 activation and in identifying and binding to prephosphorylated substrates (*110*, *111*). In addition, Rad53 is recruited by two adaptor proteins, Rad9 and Mrc1 (a functional homolog of *S. pombe* Mrc1), to be phosphorylated by mitosis entry checkpoint protein 1 (Mec1) or telomere length–regulation protein 1 (Tel1) in response to DNA-damage and replication stress (*24*, *112*–*114*). Involvement of FHA1 and FHA2 in the recruiting process remains to be firmly established, although hyperphosphorylated Rad9 preferentially binds to FHA2 (*24*), whereas both FHA1 and FHA2 are required for the Rad9-dependent activation of Rad53 (*110*, *111*, *114*, *115*). Various SQ and TQ sequences from the Rad9-SCD (from residue 390 to 458, Fig. 4B) have redundant functions in their interactions with Rad53. The K_d values of synthetic phosphopeptides encompassing the first TQ sequence (pThr^{390}) within the Rad9-SCD for FHA1 and FHA2 are 2.5 and 1.4 μM, respectively (*48*). Note that Rad9 and Mrc1 both interact with Rad53-FHA1 after the occurrence of DNA damage, as determined in a mass spectrometry–based proteome-wide study (*116*). Rad9 also functions redundantly with Mrc1, the major adaptor in replication checkpoint signaling (*112*, *113*), to facilitate Rad53 activation in the Δmrc1 mutant upon hydroxyurea-induced replication stress (*112*).

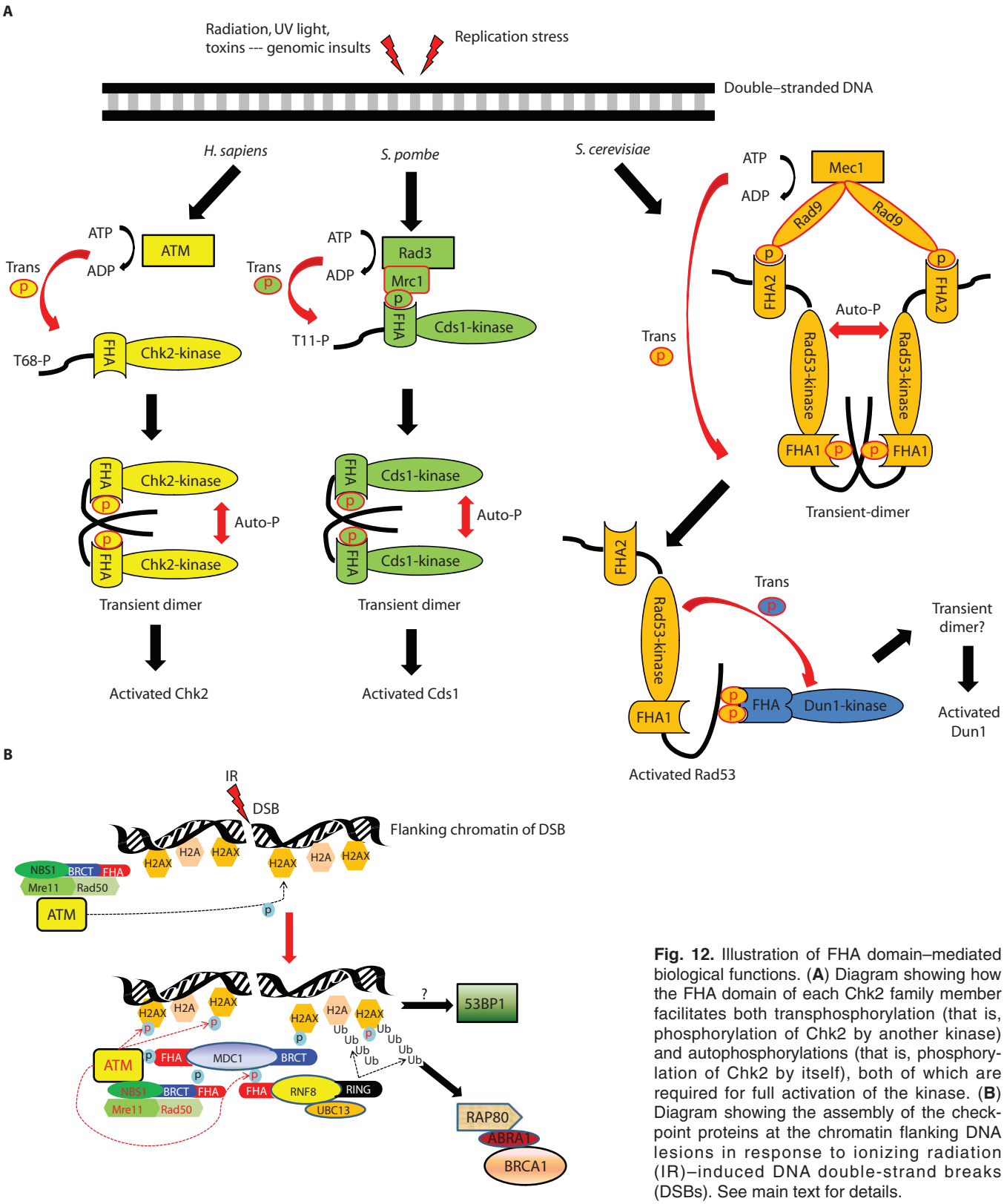

Fig. 12. Illustration of FHA domain–mediated biological functions. (**A**) Diagram showing how the FHA domain of each Chk2 family member facilitates both transphosphorylation (that is, phosphorylation of Chk2 by another kinase) and autophosphorylations (that is, phosphorylation of Chk2 by itself), both of which are required for full activation of the kinase. (**B**) Diagram showing the assembly of the checkpoint proteins at the chromatin flanking DNA lesions in response to ionizing radiation (IR)–induced DNA double-strand breaks (DSBs). See main text for details.

Species	Protein	FHA residues	pThr+3 specificity	Ref.	pThr+3 specificity (biological)	Ref.
S. cerevisiae	Rad53	573–730 (FHA2)	Ile, Leu	(*11*, *27*, *41*)	Val (Rad9)	(*48*)
S. cerevisiae	Rad53	14–164 (FHA1)	Asp	(*11*, *12*)	Ile (Mdt1), Val (Rad9), Asp(Ptc2)	(*45*, *48*, *51*)
S. cerevisiae	Dun1	19–159	None		pTXXpTXX (Rad53)	(*33*)
S. pombe	Cds1		Asp	(*11*)	–	
A. thaliana	KAPP	180–313	Ser, Ala	(*11*)	pTLVA (Bak1)	(*10*, *29*, *37*)
H. sapiens	Chk2	1–225	Ile	(*13*)	–	
H. sapiens	Ki67	1–120	None		Extended (hNIFK)	(*34*)
M. musculus	PNK	8–108	None		pT-3 (XRCC4)	(*14*)
H. sapiens	RNF8		Tyr, Phe	(*30*)	Phe (MDC1)	(*30*, *76*)
M. tuberculosis	EmbR	285–382	pT-3 to pT+3 (weak)	(*54*)	–	

Table 2. Summary of ligand specificities derived from chemical (combinatorial library) and biological approaches.

When DNA damage occurs in vivo, *S. cerevisiae* Rad53 forms dimers or oligomers, which undergo autophosphorylation (*117*). Mutations in its FHA and SCD domains compromise its intermolecular interactions and autophosphorylation activity (*55*). However, detailed molecular mechanisms of the roles of FHA1 and FHA2 in the autophosphorylation of Rad53 remain to be established. Singly phosphorylated Rad53-SCD1 phosphopeptides interact with the FHA1, but not FHA2, domain of Rad53 in vitro, with phosphorylation at Thr^5-Gln^6 or Thr^8-Gln^9 motifs having the lowest K_d values (~10 to 20 μM) (*33*). Another study (*118*) showed that the topological order of FHA1 and FHA2 is critical to the autophosphorylation of Rad53 and the downstream transcriptional activation of RNR3 (ribonucleotide reductase 3), whereas this order does not affect phosphorylation of Rad53 by upstream kinases. A mutant Rad53 with swapped FHA domains has no kinase activity, although it can still be recruited to upstream kinases in response to DNA damage. This evidence implies that the intermolecular interaction between the FHA domain and the phosphorylated SCD in a specific spatial arrangement might be critical to the dimerization- or oligomerization-driven autophosphorylation of Rad53.

Evidence is accumulating that Rad53-FHA domains mediate not only the activation, but also the inactivation, of Rad53 during cell cycle checkpoints (*45*, *110*, *111*, *114*, *115*). A return to normal growth conditions after stress-induced responses is crucial for the cell, and this occurs as a result of recovery (after DNA repair) or adaptation (the resumption of proliferation despite limited irreparable damage) (*45*). The *S. cerevisiae* phosphatases Ptc2 and Ptc3 interact with Rad53 and are involved in checkpoint inactivation in response to DSBs induced by site-specific homothallic switching endonuclease (*49*). The interaction of Ptc2 and Ptc3 with Rad53 occurs through the FHA1 domain of Rad53 in a phosphorylation-dependent manner. The K_d value for binding of the synthetic phosphopeptides encompassing $pThr^{376}$ of Ptc2 (pT^{376}DAD) to Rad53-FHA1 is 2.3 μM (*45*). In vivo, this binding occurs when Ptc2 is phosphorylated by CK2 on Thr^{376}, which leads to dephosphorylation of Rad53 and the resumption of the cell cycle after DNA damage (*45*).

Dun1. Last, but not least, is the dramatic finding of an FHA domain with two specific pThr-binding sites (*33*) (Fig. 7C). *S. cerevisiae* Dun1 is a kinase that is phosphorylated and activated by Rad53 (*119*, *120*). In vivo studies have indicated that the phosphorylated SCD1 of Rad53 interacts with Dun1-FHA (*56*) and leads Rad53 to phosphorylate Thr^{380} at the Dun1 activation loop, thus activating Dun1 (*120*) (Fig. 12A). Mutation of all four Thr residues to Ala in the TQ motifs of SCD1 abolishes the kinase activity of Rad53 and renders cells hypersensitive to DNA damage–causing reagents. The autokinase activity of Rad53 and Rad53-dependent survival in response to genotoxic stress can be restored by reverting any one of these mutated residues to Thr, whereas transduction of signals downstream of Dun1 remains retarded (*33*, *56*). In vitro binding studies also indicate that the Rad53-FHA1 recognizes and binds to singly phosphorylated Rad53-SCD1 peptides. In contrast, the Dun1-FHA domain shows strongest binding to synthetic phosphopeptides of Rad53-SCD1 that contain simultaneously phosphorylated Thr^5 and Thr^8 residues (*33*). As discussed above, the results of structural and biological studies reveal a hierarchical regulation of the Rad53-Dun1 signaling cascade by a "phospho-counting

mechanism" that involves both the Rad53-FHA1 and Dun1-FHA domains (*33*).

To date, whether and how Dun1-FHA regulates autophosphorylation of Dun1 remains elusive. A study indicated that mutations of Ser^{74} and His^{77} of the Dun1-FHA do not abolish its autokinase activity (*119*). Unlike human Chk2, *S. cerevisiae* Rad53, or *S. pombe* Cds1, the phosphorylation of Thr^{380} in the Dun1 activation loop, which activates the kinase activity of Dun1, occurs through its phosphorylation by Rad53 rather than through autophosphorylation (*120*, *121*). This raises the question of why Dun1 still needs its autophosphorylation activity. However, it appears that autophosphorylation of Dun1 does occur and that it also plays a substantial role in regulating the kinase activity of Dun1 after DNA damage, because amino acid substitutions at the Dun1 autophosphorylation sites, Ser^{10} and Ser^{139}, render cells sensitive to ultraviolet light and hydroxyurea treatment (*120*).

More than 10 Dun1-associated proteins have been identified, but the involvement of its FHA domain in these interactions is still unknown in most cases (*122*). Many of these proteins are related to the DNA-damage response, but some are not. Reverse Spt phenotype 5 (Rsp5), an E3 ubiquitin ligase, is one of the latter, and it is considered an E3 ubiquitin ligase for suppressor of Mec lethality 1 (Sml1). Two other Dun1-associated proteins, translation machinery associated (TMA29, also known as Ymr226c) and phosphorylation inhibited by long-chain bases (PIL1, also known as Ygr086C), are induced by general cell stress, rather than by the occurrence of DNA damage. In addition, it has been suggested that Dun1 may be involved in a Rad53-independent checkpoint pathway (*119*). It is possible that future studies will uncover other mechanisms of the Dun1-FHA domain in these functions.

Roles for KAPP and DDL in Growth and Development in Plants

KAPP interacts with many receptor-like protein kinases (RLKs), through its kinase-interacting FHA domain in a phosphorylation-dependent manner (*123*). These RLKs, such as CLAVATA1 (CLV1), brassinosteroid-insensitive kinase 1 (BRI1), and BRI1-associated kinase 1 (BAK1), are associated with plant growth and development and are sensor proteins that trigger signaling cascades in response to changing environmental conditions. One study has shown that KAPP attenuates CLV1 activity in plant development (*124*). The interaction between KAPP and RLKs implicates FHA domains in signal transduction pathways of plants and, hence, in the regulation of plant development, environmental responses, and adaptation (*29*). Additionally, dawdle (ddl) plants with insertional mutations in the genes encoding other FHA domain–containing proteins of *Arabidopsis thaliana* show delayed development and defective roots, shoots, and flowers (*125*). The FHA domain–containing protein DAWDLE (DDL) plays a role in the biogenesis of microRNAs (miRNAs) and endogenous siRNAs (*126*). The FHA domain of DDL mediates its interaction with DICER-LIKE1 (DCL1), a protein that processes the conversion of pre-miRNAs to mature miRNAs in the nucleus (*126*). Smad nuclear interacting protein 1 (SNIP1), another FHA domain–containing protein and a human homolog of DDL, was also shown to perform a similar function, hence highlighting their conserved roles in miRNA biogenesis (*126*). The FHA domain–containing transcription activator NtFHA1 in *Nicotiana tabacum*, a likely functional analog of Fhl1 in yeast, was suggested to regulate cell growth and ribosomal RNA processing (*127*).

Role for EmbR in Bacterial Regulatory Pathways

Phosphorylation of proteins and enzymes by Ser-Thr protein kinases is a major means by which prokaryotic signaling mechanisms are regulated (*128*, *129*). A comprehensive search and survey of bacterial FHA domains highlighted their possible roles in various processes, including regulation of cell shape, sporulation, transport, signal transduction, and ethambutol (Emb) resistance (*130*). Emb is a frontline antimycobacterial drug that targets the mycobacterial cell wall. A number of membrane-embedded arabinosyltransferases (encoded in the EmbCAB gene cluster) are involved in the synthesis of arabinogalactan and lipoarabinomannan, critical components of the mycobacterial cell wall (*131*). Expression of the genes encoding these arabinosyltransferases is positively regulated by the *embR* gene, which plays a role in resistance to Emb by modulating the activity level of the Emb-resistant arabinosyltransferase (*132*). Because deletion mutants of the stress-response Ser-Thr protein kinase PknH inhibit the expression of the *emb* genes, this indicates that bacterial cell wall synthesis and, hence, cell growth are controlled through a PknH-dependent pathway (*133*). The FHA domain–containing protein EmbR interacts with PknH in a phosphorylation-dependent manner and functions downstream of PknH, which implicates its FHA domain in the regulation of *emb* genes and thus in mycobacterial cell wall synthesis (*54*). EmbR has an N-terminal DNA binding domain, a bacterial transcriptional activation domain, and a C-terminal FHA domain, whose structure has been reported (*54*).

Future Perspectives

Despite the wealth of structural and functional information available, we are probably still at the early stage of a full understanding of the biological functions of FHA domains and of the structural bases of these functions. Even if a biological binding partner is clearly identified, the phosphorylation site(s) for binding by the FHA domain will need to be characterized. The next step will be to identify the kinase that phosphorylates this site. Subsequent preparation of the appropriate phosphoprotein for structural studies of protein-phosphoprotein complexes will also be a daunting task; the best that has been achieved so far is the preparation of a complex of Ki67-FHA and a phosphorylated 45–amino acid–residue fragment. Another important question is whether the phospho-counting signaling mechanism demonstrated in the Rad53-Dun1 cascade is shared in other signaling pathways involving FHA or other domains. Further advancement of these studies is a clear direction for FHA domain research in the next decade.

References and Notes

1. K. Hofmann, P. Bucher, The FHA domain: A putative nuclear signalling domain found in protein kinases and transcription factors. *Trends Biochem. Sci.* **20**, 347–349 (1995).
2. M. Toyota, Y. Sasaki, A. Satoh, K. Ogi, T. Kikuchi, H. Suzuki, H. Mita, N. Tanaka, F. Itoh, J. P. Issa, K. W. Jair, K. E. Schuebel, K. Imai, T. Tokino, Epigenetic inactivation of CHFR in human tumors. *Proc. Natl. Acad. Sci. U.S.A.* **100**, 7818–7823 (2003).
3. C. K. Ea, L. Sun, J. Inoue, Z. J. Chen, TIFA activates IκB kinase (IKK) by promoting oligomerization and ubiquitination of TRAF6. *Proc. Natl. Acad. Sci. U.S.A.* **101**, 15318–15323 (2004).
4. N. Uhrhammer, J. O. Bay, S. Gosse-Brun, F. Kwiatkowski, P. Rio, A. Daver, Y. J. Bignon, Allelic imbalance at NBS1 is frequent in both proximal and distal colorectal carcinoma. *Oncol. Rep.* **7**, 427–431 (2000).
5. Single-letter abbreviations for the amino acid residues are as follows: A, Ala; C, Cys; D, Asp; E, Glu; F, Phe; G, Gly; H, His; I, Ile; K, Lys; L, Leu; M, Met; N, Asn; P, Pro; Q, Gln; R, Arg; S, Ser; T, Thr; V, Val; W, Trp; Y, Tyr; and X, any amino acid.
6. D. Durocher, S. P. Jackson, The FHA domain. *FEBS Lett.* **513**, 58–66 (2002).

7. A. Hammet, B. L. Pike, C. J. McNees, L. A. Conlan, N. Tenis, J. Heierhorst, FHA domains as phospho-threonine binding modules in cell signaling. *IUBMB Life* **55**, 23–27 (2003).
8. H. Liao, I. J. Byeon, M. D. Tsai, Structure and function of a new phosphopeptide-binding domain containing the FHA2 of Rad53. *J. Mol. Biol.* **294**, 1041–1049 (1999).
9. A. Hammet, B. L. Pike, K. I. Mitchelhill, T. Teh, B. Kobe, C. M. House, B. E. Kemp, J. Heierhorst, FHA domain boundaries of the Dun1p and Rad53p cell cycle checkpoint kinases. *FEBS Lett.* **471**, 141–146 (2000).
10. G. I. Lee, Z. Ding, J. C. Walker, S. R. Van Doren, NMR structure of the forkhead-associated domain from the *Arabidopsis* receptor kinase-associated protein phosphatase. *Proc. Natl. Acad. Sci. U.S.A.* **100**, 11261–11266 (2003).
11. D. Durocher, I. A. Taylor, D. Sarbassova, L. F. Haire, S. L. Westcott, S. P. Jackson, S. J. Smerdon, M. B. Yaffe, The molecular basis of FHA domain:phosphopeptide binding specificity and implications for phospho-dependent signaling mechanisms. *Mol. Cell* **6**, 1169–1182 (2000).
12. H. Liao, C. Yuan, M. I. Su, S. Yongkiettrakul, D. Qin, H. Li, I. J. Byeon, D. Pei, M. D. Tsai, Structure of the FHA1 domain of yeast Rad53 and identification of binding sites for both FHA1 and its target protein Rad9. *J. Mol. Biol.* **304**, 941–951 (2000).
13. J. Li, B. L. Williams, L. F. Haire, M. Goldberg, E. Wilker, D. Durocher, M. B. Yaffe, S. P. Jackson, S. J. Smerdon, Structural and functional versatility of the FHA domain in DNA-damage signaling by the tumor suppressor kinase Chk2. *Mol. Cell* **9**, 1045–1054 (2002).
14. N. K. Bernstein, R. S. Williams, M. L. Rakovszky, D. Cui, R. Green, F. Karimi-Busheri, R. S. Mani, S. Galicia, C. A. Koch, C. E. Cass, D. Durocher, M. Weinfeld, J. N. Glover, The molecular architecture of the mammalian DNA repair enzyme, polynucleotide kinase. *Mol. Cell* **17**, 657–670 (2005).
15. E. S. Stavridi, Y. Huyen, I. R. Loreto, D. M. Scolnick, T. D. Halazonetis, N. P. Pavletich, P. D. Jeffrey, Crystal structure of the FHA domain of the Chfr mitotic checkpoint protein and its complex with tungstate. *Structure* **10**, 891–899 (2002).
16. X. Xu, L. M. Tsvetkov, D. F. Stern, Chk2 activation and phosphorylation-dependent oligomerization. *Mol. Cell. Biol.* **22**, 4419–4432 (2002).
17. C. S. Gilbert, C. M. Green, N. F. Lowndes, Budding yeast Rad9 is an ATP-dependent Rad53 activating machine. *Mol. Cell* **8**, 129–136 (2001).
18. J. Y. Ahn, X. Li, H. L. Davis, C. E. Canman, Phosphorylation of threonine 68 promotes oligomerization and autophosphorylation of the Chk2 protein kinase via the forkhead-associated domain. *J. Biol. Chem.* **277**, 19389–19395 (2002).
19. G. Wu, Y.-G. Chen, B. Ozdamar, C. A. Gyuricza, P. A. Chong, J. L. Wrana, J. Massagué, Y. Shi, Structural basis of Smad2 recognition by the Smad anchor for receptor activation. *Science* **287**, 92–97 (2000).
20. M. Huse, T. W. Muir, L. Xu, Y.-G. Chen, J. Kuriyan, J. Massagu, T. G. F. The, β receptor activation process: An inhibitor- to substrate-binding switch. *Mol. Cell* **8**, 671–682 (2001).
21. S. Zhou, S. E. Shoelson, M. Chaudhuri, G. Gish, T. Pawson, W. G. Haser, F. King, T. Roberts, S. Ratnofsky, R. J. Lechleider, B. G. Neel, R. B. Birge, J. E. Fajardo, M. M. Chou, H. Hanafusa, B. Schaffhausen, L. C. Cantley, SH2 domains recognize specific phosphopeptide sequences. *Cell* **72**, 767–778 (1993).
22. M. B. Yaffe, S. J. Smerdon, The use of in vitro peptide-library screens in the analysis of phosphoserine/threonine-binding domain structure and function. *Annu. Rev. Biophys. Biomol. Struct.* **33**, 225–244 (2004).
23. D. Durocher, J. Henckel, A. R. Fersht, S. P. Jackson, The FHA domain is a modular phosphopeptide recognition motif. *Mol. Cell* **4**, 387–394 (1999).
24. Z. Sun, J. Hsiao, D. S. Fay, D. F. Stern, Rad53 FHA domain associated with phosphorylated Rad9 in the DNA damage checkpoint. *Science* **281**, 272–274 (1998).
25. J. M. Stone, M. A. Collinge, R. D. Smith, M. A. Horn, J. C. Walker, Interaction of a protein phosphatase with an *Arabidopsis* serine-threonine receptor kinase. *Science* **266**, 793–795 (1994).
26. J. Li, G. P. Smith, J. C. Walker, Kinase interaction domain of kinase-associated protein phosphatase, a phosphoprotein-binding domain. *Proc. Natl. Acad. Sci. U.S.A.* **96**, 7821–7826 (1999).
27. P. Wang, I. J. Byeon, H. Liao, K. D. Beebe, S. Yongkiettrakul, D. Pei, M. D. Tsai, II, Structure and specificity of the interaction between the FHA2 domain of rad53 and phosphotyrosyl peptides. *J. Mol. Biol.* **302**, 927–940 (2000).
28. J. Li, G. I. Lee, S. R. Van Doren, J. C. Walker, The FHA domain mediates phosphoprotein interactions. *J. Cell Sci.* **113**, 4143–4149 (2000).
29. Z. Ding, H. Wang, X. Liang, E. R. Morris, F. Gallazzi, S. Pandit, J. Skolnick, J. C. Walker, S. R. Van Doren, Phosphoprotein and phosphopeptide interactions with the FHA domain from *Arabidopsis* kinase-associated protein phosphatase. *Biochemistry* **46**, 2684–2696 (2007).
30. M. S. Huen, R. Grant, I. Manke, K. Minn, X. Yu, M. B. Yaffe, J. Chen, RNF8 transduces the DNA-damage signal via histone ubiquitylation and checkpoint protein assembly. *Cell* **131**, 901–914 (2007).
31. D. Qin, H. Lee, C. Yuan, Y. Ju, M. D. Tsai, Identification of potential binding sites for the FHA domain of human Chk2 by in vitro binding studies. *Biochem. Biophys. Res. Commun.* **311**, 803–808 (2003).
32. C. Yuan, S. Yongkiettrakul, I. J. Byeon, S. Zhou, M. D. Tsai, Solution structures of two FHA1-phosphothreonine peptide complexes provide insight into the structural basis of the ligand specificity of FHA1 from yeast Rad53. *J. Mol. Biol.* **314**, 563–575 (2001).
33. H. Lee, C. Yuan, A. Hammet, A. Mahajan, E. S. Chen, M. R. Wu, M. I. Su, J. Heierhorst, M. D. Tsai, Diphosphothreonine-specific interaction between an SQ/TQ cluster and an FHA domain in the Rad53-Dun1 kinase cascade. *Mol. Cell* **30**, 767–778 (2008).
34. I. J. Byeon, H. Li, H. Song, A. M. Gronenborn, M. D. Tsai, Sequential phosphorylation and multisite interactions characterize specific target recognition by the FHA domain of Ki67. *Nat. Struct. Mol. Biol.* **12**, 987–993 (2005).
35. H. Kumeta, K. Ogura, S. Adachi, Y. Fujioka, N. Tanuma, K. Kikuchi, F. Inagaki, The NMR structure of the NIPP1 FHA domain. *J. Biomol. NMR* **40**, 219–224 (2008).
36. I. J. Byeon, S. Yongkiettrakul, M. D. Tsai, Solution structure of the yeast Rad53 FHA2 complexed with a phosphothreonine peptide pTXXL: Comparison with the structures of FHA2-pYXL and FHA1-pTXXD complexes. *J. Mol. Biol.* **314**, 577–588 (2001).
37. Z. Ding, G. I. Lee, X. Liang, F. Gallazzi, A. Arunima, S. R. Van Doren, PhosphoThr peptide binding globally rigidifies much of the FHA domain from *Arabidopsis* receptor kinase-associated protein phosphatase. *Biochemistry* **44**, 10119–10134 (2005).
38. J. Gerdes, U. Schwab, H. Lemke, H. Stein, Production of a mouse monoclonal antibody reactive with a human nuclear antigen associated with cell proliferation. *Int. J. Cancer* **31**, 13–20 (1983).
39. Z. Zhou, S. J. Elledge, DUN1 encodes a protein kinase that controls the DNA damage response in yeast. *Cell* **75**, 1119–1127 (1993).
40. H. Li, I. J. Byeon, Y. Ju, M. D. Tsai, Structure of human Ki67 FHA domain and its binding to a phosphoprotein fragment from hNIFK reveal unique recognition sites and new views to the structural basis of FHA domain functions. *J. Mol. Biol.* **335**, 371–381 (2004).
41. S. Yongkiettrakul, I. J. Byeon, M. D. Tsai, The ligand specificity of yeast Rad53 FHA domains at the +3 position is determined by nonconserved residues. *Biochemistry* **43**, 3862–3869 (2004).
42. S. Miyamoto, P. A. Kollman, What determines the strength of noncovalent association of ligands to proteins in aqueous solution? *Proc. Natl. Acad. Sci. U.S.A.* **90**, 8402–8406 (1993).
43. S. Miyamoto, P. A. Kollman, Absolute and relative binding free energy calculations of the interaction of biotin and its analogs with streptavidin using molecular dynamics/free energy perturbation approaches. *Proteins* **16**, 226–245 (1993).
44. P. Y. Huang, R. G. Carbonell, Affinity chromatographic screening of soluble combinatorial peptide libraries. *Biotechnol. Bioeng.* **63**, 633–641 (1999).
45. G. Guillemain, E. Ma, S. Mauger, S. Miron, R. Thai, R. Guerois, F. Ochsenbein, M. C. Marsolier-Kergoat, Mechanisms of checkpoint kinase Rad53 inactivation after a double-strand break in *Saccharomyces cerevisiae*. *Mol. Cell. Biol.* **27**, 3378–3389 (2007).
46. Y. Xu, M. Davenport, T. J. Kelly, Two-stage mechanism for activation of the DNA replication checkpoint kinase Cds1 in fission yeast. *Genes Dev.* **20**, 990–1003 (2006).
47. Z. Lou, K. Minter-Dykhouse, X. Wu, J. Chen, MDC1 is coupled to activated CHK2 in mammalian DNA damage response pathways. *Nature* **421**, 957–961 (2003).
48. M. F. Schwartz, J. K. Duong, Z. Sun, J. S. Morrow, D. Pradhan, D. F. Stern, Rad9 phosphorylation sites couple Rad53 to the *Saccharomyces cerevisiae* DNA damage checkpoint. *Mol. Cell* **9**, 1055–1065 (2002).
49. C. Leroy, S. E. Lee, M. B. Vaze, F. Ochsenbien, R. Guerois, J. E. Haber, M.-C. Marsolier-Kergoat, PP2C phosphatases Ptc2 and Ptc3 are required for DNA checkpoint inactivation after a double-strand break. *Mol. Cell* **11**, 827–835 (2003).
50. B. L. Pike, S. Yongkiettrakul, M. D. Tsai, J. Heierhorst, Mdt1, a novel Rad53 FHA1 domain-interacting protein, modulates DNA damage tolerance and G_2/M cell cycle progression in *Saccharomyces cerevisiae*. *Mol. Cell. Biol.* **24**, 2779–2788 (2004).
51. A. Mahajan, C. Yuan, B. L. Pike, J. Heierhorst, C. F. Chang, M. D. Tsai, FHA domain-ligand interactions: Importance of integrating chemical and biological approaches. *J. Am. Chem. Soc.* **127**, 14572–14573 (2005).
52. K. Tanaka, P. Russell, Cds1 phosphorylation by Rad3-Rad26 kinase is mediated by forkhead-associated domain interaction with Mrc1. *J. Biol. Chem.* **279**, 32079–32086 (2004).
53. K. Tanaka, M. N. Boddy, X.-B. Chen, C. H. McGowan, P. Russell, Threonine-11, phosphorylated by Rad3 and ATM in vitro, is required for activation of fission yeast checkpoint kinase Cds1. *Mol. Cell. Biol.* **21**, 3398–3404 (2001).
54. L. J. Alderwick, V. Molle, L. Kremer, A. J. Cozzone, T. R. Dafforn, G. S. Besra, K. Futterer, Molecular structure of EmbR, a response element of Ser/Thr kinase signaling in *Mycobac-*

terium tuberculosis. *Proc. Natl. Acad. Sci. U.S.A.* **103**, 2558–2563 (2006).
55. N. Jia-Lin Ma, D. F. Stern, Regulation of the Rad53 protein kinase in signal amplification by oligomer assembly and disassembly. *Cell Cycle* **7**, 808–817 (2008).
56. S.-J. Lee, M. F. Schwartz, J. K. Duong, D. F. Stern, Rad53 phosphorylation site clusters are important for Rad53 regulation and signaling. *Mol. Cell. Biol.* **23**, 6300–6314 (2003).
57. T. Scholzen, J. Gerdes, The Ki-67 protein: From the known and the unknown. *J. Cell. Physiol.* **182**, 311–322 (2000).
58. M. Takagi, Y. Matsuoka, T. Kurihara, Y. Yoneda, Chmadrin: A novel Ki-67 antigen-related perichromosomal protein possibly implicated in higher order chromatin structure. *J. Cell Sci.* **112**, 2463–2472 (1999).
59. M. Takagi, M. Sueishi, T. Saiwaki, A. Kametaka, Y. Yoneda, A novel nucleolar protein, NIFK, interacts with the forkhead associated domain of Ki-67 antigen in mitosis. *J. Biol. Chem.* **276**, 25386–25391 (2001).
60. M. Sueishi, M. Takagi, Y. Yoneda, The forkhead-associated domain of Ki-67 antigen interacts with the novel kinesin-like protein Hklp2. *J. Biol. Chem.* **275**, 28888–28892 (2000).
61. J. C. Obenauer, L. C. Cantley, M. B. Yaffe, Scansite 2.0: Proteome-wide prediction of cell signaling interactions using short sequence motifs. *Nucleic Acids Res.* **31**, 3635–3641 (2003).
62. D. Bridges, G. B. Moorhead, 14-3-3 proteins: A number of functions for a numbered protein. *Sci. STKE* **2005**, re10 (2005).
63. J. R. Engen, T. E. Wales, J. M. Hochrein, M. A. Meyn, 3rd, S. Banu Ozkan, I. Bahar, T. E. Smithgall, Structure and dynamic regulation of Src-family kinases. *Cell. Mol. Life Sci.* **65**, 3058–3073 (2008).
64. A. Zarrinpar, R. P. Bhattacharyya, W. A. Lim, The structure and function of proline recognition domains. *Sci. STKE* **2003**, re8 (2003).
65. J. Bartek, J. Falck, J. Lukas, Chk2 kinase—a busy messenger. *Nat. Rev. Mol. Cell Biol.* **2**, 877–886 (2001).
66. J.-Y. Ahn, J. K. Schwarz, H. Piwnica-Worms, C. E. Canman, Threonine 68 phosphorylation by ataxia telangiectasia mutated is required for efficient activation of Chk2 in response to ionizing radiation. *Cancer Res.* **60**, 5934–5936 (2000).
67. M. J. Henderson, M. A. Munoz, D. N. Saunders, J. L. Clancy, A. J. Russell, B. Williams, D. Pappin, K. K. Khanna, S. P. Jackson, R. L. Sutherland, C. K. W. Watts, EDD mediates DNA damage-induced activation of CHK2. *J. Biol. Chem.* **281**, 39990–40000 (2006).
68. D. W. Bell, J. M. Varley, T. E. Szydlo, D. H. Kang, D. C. R. Wahrer, K. E. Shannon, M. Lubratovich, S. J. Verselis, K. J. Isselbacher, J. F. Fraumeni, J. M. Birch, F. P. Li, J. E. Garber, D. A. Haber, Heterozygous germ line hCHK2 mutations in Li-Fraumeni syndrome. *Science* **286**, 2528–2531 (1999).
69. N. Sodha, T. S. Mantoni, S. V. Tavtigian, R. Eeles, M. D. Garrett, Rare germ line CHEK2 variants identified in breast cancer families encode proteins that show impaired activation. *Cancer Res.* **66**, 8966–8970 (2006).
70. S. B. Lee, S. H. Kim, D. W. Bell, D. C. R. Wahrer, T. A. Schiripo, M. M. Jorczak, D. C. Sgroi, J. E. Garber, F. P. Li, K. E. Nichols, J. M. Varley, A. K. Godwin, K. M. Shannon, E. Harlow, D. A. Haber, Destabilization of CHK2 by a missense mutation associated with Li-Fraumeni syndrome. *Cancer Res.* **61**, 8062–8067 (2001).
71. X. Wu, S. R. Webster, J. Chen, Characterization of tumor-associated Chk2 mutations. *J. Biol. Chem.* **276**, 2971–2974 (2001).
72. J. Falck, C. Lukas, M. Protopopova, J. Lukas, G. Selivanova, J. Bartek, Functional impact of concomitant versus alternative defects in the Chk2-p53 tumour suppressor pathway. *Oncogene* **20**, 5503–5510 (2001).
73. J. Falck, N. Mailand, R. G. Syljuasen, J. Bartek, J. Lukas, The ATM-Chk2-Cdc25A checkpoint pathway guards against radioresistant DNA synthesis. *Nature* **410**, 842–847 (2001).
74. B. Wang, S. J. Elledge, Ubc13/Rnf8 ubiquitin ligases control foci formation of the Rap80/Abraxas/Brca1/Brcc36 complex in response to DNA damage. *Proc. Natl. Acad. Sci. U.S.A.* **104**, 20759–20763 (2007).
75. N. Mailand, S. Bekker-Jensen, H. Faustrup, F. Melander, J. Bartek, C. Lukas, J. Lukas, RNF8 ubiquitylates histones at DNA double-strand breaks and promotes assembly of repair proteins. *Cell* **131**, 887–900 (2007).
76. N. K. Kolas, J. R. Chapman, S. Nakada, J. Ylanko, R. Chahwan, F. D. Sweeney, S. Panier, M. Mendez, J. Wildenhain, T. M. Thomson, L. Pelletier, S. P. Jackson, D. Durocher, Orchestration of the DNA-damage response by the RNF8 ubiquitin ligase. *Science* **318**, 1637–1640 (2007).
77. R. Varon, C. Vissinga, M. Platzer, K. M. Cerosaletti, K. H. Chrzanowska, K. Saar, G. Beckmann, E. Seemanov, P. R. Cooper, N. J. Nowak, M. Stumm, C. M. R. Weemaes, R. A. Gatti, R. K. Wilson, M. Digweed, A. Rosenthal, K. Sperling, P. Concannon, A. Reis, Nibrin, a novel DNA double-strand break repair protein, is mutated in Nijmegen breakage syndrome. *Cell* **93**, 467–476 (1998).
78. J. P. Carney, R. S. Maser, H. Olivares, E. M. Davis, M. Le Beau, J. R. Yates, L. Hays, W. F. Morgan, J. H. J. Petrini, The hMre11/hRad50 protein complex and Nijmegen breakage syndrome: Linkage of double-strand break repair to the cellular DNA damage response. *Cell* **93**, 477–486 (1998).
79. T. H. Stracker, J.-W. F. Theunissen, M. Morales, J. H. J. Petrini, The Mre11 complex and the metabolism of chromosome breaks: The importance of communicating and holding things together. *DNA Repair (Amsterdam)* **3**, 845–854 (2004).
80. E. Olson, C. J. Nievera, A. Y.-L. Lee, L. Chen, X. Wu, The Mre11-Rad50-Nbs1 complex acts both upstream and downstream of ataxia telangiectasia mutated and Rad3-related protein (ATR) to regulate the S-phase checkpoint following UV treatment. *J. Biol. Chem.* **282**, 22939–22952 (2007).
81. S. Difilippantonio, A. Celeste, O. Fernandez-Capetillo, H. T. Chen, B. Reina San Martin, F. Van Laethem, Y. P. Yang, G. V. Petukhova, M. Eckhaus, L. Feigenbaum, K. Manova, M. Kruhlak, R. D. Camerini-Otero, S. Sharan, M. Nussenzweig, A. Nussenzweig, Role of Nbs1 in the activation of the Atm kinase revealed in humanized mouse models. *Nat. Cell Biol.* **7**, 675–685 (2005).
82. J. H. Lee, T. T. Paull, ATM activation by DNA double-strand breaks through the Mre11-Rad50-Nbs1 complex. *Science* **308**, 551–554 (2005).
83. A. Kinner, W. Wu, C. Staudt, G. Iliakis, γ-H2AX in recognition and signaling of DNA double-strand breaks in the context of chromatin. *Nucleic Acids Res.* **36**, 5678–5694 (2008).
84. M. Stucki, J. A. Clapperton, D. Mohammad, M. B. Yaffe, S. J. Smerdon, S. P. Jackson, MDC1 directly binds phosphorylated histone H2AX to regulate cellular responses to DNA double-strand breaks. *Cell* **123**, 1213–1226 (2005).
85. C. Spycher, E. S. Miller, K. Townsend, L. Pavic, N. A. Morrice, P. Janscak, G. S. Stewart, M. Stucki, Constitutive phosphorylation of MDC1 physically links the MRE11-RAD50-NBS1 complex to damaged chromatin. *J. Cell Biol.* **181**, 227–240 (2008).
86. F. Melander, S. Bekker-Jensen, J. Falck, J. Bartek, N. Mailand, J. Lukas, Phosphorylation of SDT repeats in the MDC1 N terminus triggers retention of NBS1 at the DNA damage-modified chromatin. *J. Cell Biol.* **181**, 213–226 (2008).
87. C. Xu, L. Wu, G. Cui, M. V. Botuyan, J. Chen, G. Mer, Structure of a second BRCT domain identified in the Nijmegen breakage syndrome protein Nbs1 and its function in an MDC1-dependent localization of Nbs1 to DNA damage sites. *J. Mol. Biol.* **381**, 361–372 (2008).
88. L. Wu, K. Luo, Z. Lou, J. Chen, MDC1 regulates intra-S-phase checkpoint by targeting NBS1 to DNA double-strand breaks. *Proc. Natl. Acad. Sci. U.S.A.* **105**, 11200–11205 (2008).
89. Z. Lou, K. Minter-Dykhouse, S. Franco, M. Gostissa, M. A. Rivera, A. Celeste, J. P. Manis, J. van Deursen, A. Nussenzweig, T. T. Paull, F. W. Alt, J. Chen, MDC1 maintains genomic stability by participating in the amplification of ATM-dependent DNA damage signals. *Mol. Cell* **21**, 187–200 (2006).
90. M. Goldberg, M. Stucki, J. Falck, D. D'Amours, D. Rahman, D. Pappin, J. Bartek, S. P. Jackson, MDC1 is required for the intra-S-phase DNA damage checkpoint. *Nature* **421**, 952–956 (2003).
91. G. S. Stewart, B. Wang, C. R. Bignell, A. M. Taylor, S. J. Elledge, MDC1 is a mediator of the mammalian DNA damage checkpoint. *Nature* **421**, 961–966 (2003).
92. R. S. Williams, G. Moncalian, J. S. Williams, Y. Yamada, O. Limbo, D. S. Shin, L. M. Groocock, D. Cahill, C. Hitomi, G. Guenther, D. Moiani, J. P. Carney, P. Russell, J. A. Tainer, Mre11 dimers coordinate DNA end bridging and nuclease processing in double-strand-break repair. *Cell* **135**, 97–109 (2008).
93. R. Kanaar, C. Wyman, DNA repair by the MRN complex: break it to make it. *Cell* **135**, 14–16 (2008).
94. J. Buis, Y. Wu, Y. Deng, J. Leddon, G. Westfield, M. Eckersdorff, J. M. Sekiguchi, S. Chang, D. O. Ferguson, Mre11 nuclease activity has essential roles in DNA repair and genomic stability distinct from ATM activation. *Cell* **135**, 85–96 (2008).
95. C. Chappell, L. A. Hanakahi, F. Karimi-Busheri, M. Weinfeld, S. C. West, Involvement of human polynucleotide kinase in double-strand break repair by non-homologous end joining. *EMBO J.* **21**, 2827–2832 (2002).
96. C. A. Koch, R. Agyei, S. Galicia, P. Metalnikov, P. O'Donnell, A. Starostine, M. Weinfeld, D. Durocher, Xrcc4 physically links DNA end processing by polynucleotide kinase to DNA ligation by DNA ligase IV. *EMBO J.* **23**, 3874–3885 (2004).
97. J. I. Loizou, S. F. El-Khamisy, A. Zlatanou, D. J. Moore, D. W. Chan, J. Qin, S. Sarno, F. Meggio, L. A. Pinna, K. W. Caldecott, The protein kinase CK2 facilitates repair of chromosomal DNA single-strand breaks. *Cell* **117**, 17–28 (2004).
98. N. Gueven, O. J. Becherel, A. W. Kijas, P. Chen, O. Howe, J. H. Rudolph, R. Gatti, H. Date, O. Onodera, G. Taucher-Scholz, M. F. Lavin, Aprataxin, a novel protein that protects against genotoxic stress. *Hum. Mol. Genet.* **13**, 1081–1093 (2004).
99. H. Luo, D. W. Chan, T. Yang, M. Rodriguez, B. P. Chen, M. Leng, J. J. Mu, D. Chen, Z. Songyang, Y. Wang, J. Qin, A new XRCC1-containing complex and its role in cellular survival of methyl methanesulfonate treatment. *Mol. Cell. Biol.* **24**, 8356–8365 (2004).
100. P. M. Clements, C. Breslin, E. D. Deeks, P. J. Byrd, L. Ju, P. Bieganowski, C. Brenner, M. C. Moreira, A. M. Taylor, K. W. Caldecott, The

ataxia-oculomotor apraxia 1 gene product has a role distinct from ATM and interacts with the DNA strand break repair proteins XRCC1 and XRCC4. *DNA Repair (Amsterdam)* **3**, 1493–1502 (2004).
101. S. Kanno, H. Kuzuoka, S. Sasao, Z. Hong, L. Lan, S. Nakajima, A. Yasui, A novel human AP endonuclease with conserved zinc-finger-like motifs involved in DNA strand break responses. *EMBO J.* **26**, 2094–2103 (2007).
102. N. Iles, S. Rulten, S. F. El-Khamisy, K. W. Caldecott, APLF (C2orf13) is a novel human protein involved in the cellular response to chromosomal DNA strand breaks. *Mol. Cell. Biol.* **27**, 3793–3803 (2007).
103. H. Zhao, K. Tanaka, E. Nogochi, C. Nogochi, P. Russell, Replication checkpoint protein Mrc1 is regulated by Rad3 and Tel1 in fission yeast. *Mol. Cell. Biol.* **23**, 8395–8403 (2003).
104. M. Kai, M. N. Boddy, P. Russell, T. S. F. Wang, Replication checkpoint kinase Cds1 regulates Mus81 to preserve genome integrity during replication stress. *Genes Dev.* **19**, 919–932 (2005).
105. J. B. Allen, Z. Zhou, W. Siede, E. C. Friedberg, S. J. Elledge, The SAD1/RAD53 protein kinase controls multiple checkpoints and DNA damage-induced transcription in yeast. *Genes Dev.* **8**, 2401–2415 (1994).
106. T. A. Weinert, G. L. Kiser, L. H. Hartwell, Mitotic checkpoint genes in budding yeast and the dependence of mitosis on DNA replication and repair. *Genes Dev.* **8**, 652–665 (1994).
107. K. Shirahige, Y. Hori, K. Shiraishi, M. Yamashita, K. Takahashi, C. Obuse, T. Tsurimoto, H. Yoshikawa, Regulation of DNA-replication origins during cell-cycle progression. *Nature* **395**, 618–621 (1998).
108. S. Kim, T. A. Weinert, Characterization of the checkpoint gene RAD53/MEC2 in *Saccharomyces cerevisiae*. *Yeast* **13**, 735–745 (1997).
109. M. P. Longhese, V. Paciotti, H. Neecke, G. Lucchini, Checkpoint proteins influence telomeric silencing and length maintenance in budding yeast. *Genetics* **155**, 1577–1591 (2000).
110. M. F. Schwartz, S. J. Lee, J. K. Duong, S. Eminaga, D. F. Stern, FHA domain-mediated DNA checkpoint regulation of Rad53. *Cell Cycle* **2**, 384–396 (2003).
111. B. L. Pike, S. Yongkiettrakul, M.-D. Tsai, J. Heierhorst, Diverse but overlapping functions of the two forkhead-associated (FHA) domains in Rad53 checkpoint kinase activation. *J. Biol. Chem.* **278**, 30421–30424 (2003).
112. A. A. Alcasabas, A. J. Osborn, J. Bachant, F. Hu, P. J. Werler, K. Bousset, K. Furuya, J. F. Diffley, A. M. Carr, S. J. Elledge, Mrc1 transduces signals of DNA replication stress to activate Rad53. *Nat. Cell Biol.* **3**, 958–965 (2001).
113. A. J. Osborn, S. J. Elledge, Mrc1 is a replication fork component whose phosphorylation in response to DNA replication stress activates Rad53. *Genes Dev.* **17**, 1755–1767 (2003).
114. F. D. Sweeney, F. Yang, A. Chi, J. Shabanowitz, D. F. Hunt, D. Durocher, *Saccharomyces cerevisiae* Rad9 acts as a Mec1 adaptor to allow Rad53 activation. *Curr. Biol.* **15**, 1364–1375 (2005).
115. B. L. Pike, N. Tenis, J. Heierhorst, Rad53 kinase activation-independent replication checkpoint function of the N-terminal forkhead-associated (FHA1) domain. *J. Biol. Chem.* **279**, 39636–39644 (2004).
116. M. B. Smolka, S.-h. Chen, P. S. Maddox, J. M. Enserink, C. P. Albuquerque, X. X. Wei, A. Desai, R. D. Kolodner, H. Zhou, An FHA domain-mediated protein interaction network of Rad53 reveals its role in polarized cell growth. *J. Cell Biol.* **175**, 743–753 (2006).
117. J.-L. Ma, S.-J. Lee, J. K. Duong, D. F. Stern, Activation of the checkpoint kinase Rad53 by the phosphatidyl inositol kinase-like kinase Mec1. *J. Biol. Chem.* **281**, 3954–3963 (2006).
118. A. T. Y. Tam, B. L. Pike, J. Heierhorst, Location-specific functions of the two forkhead-associated domains in Rad53 checkpoint kinase signaling. *Biochemistry* **47**, 3912–3916 (2008).
119. V. I. Bashkirov, E. V. Bashkirova, E. Haghnazari, W.-D. Heyer, Direct kinase-to-kinase signaling mediated by the FHA phosphoprotein recognition domain of the Dun1 DNA damage checkpoint kinase. *Mol. Cell. Biol.* **23**, 1441–1452 (2003).
120. S. H. Chen, M. B. Smolka, H. Zhou, Mechanism of Dun1 activation by Rad53 phosphorylation in *Saccharomyces cerevisiae*. *J. Biol. Chem.* **282**, 986–995 (2007).
121. A. Krupa, G. Preethi, N. Srinivasan, Structural modes of stabilization of permissive phosphorylation sites in protein kinases: Distinct strategies in Ser/Thr and Tyr kinases. *J. Mol. Biol.* **339**, 1025–1039 (2004).
122. Y. Ho, A. Gruhler, A. Heilbut, G. D. Bader, L. Moore, S.-L. Adams, A. Millar, P. Taylor, K. Bennett, K. Boutilier, L. Yang, C. Wolting, I. Donaldson, S. Schandorff, J. Shewnarane, M. Vo, J. Taggart, M. Goudreault, B. Muskat, C. Alfarano, D. Dewar, Z. Lin, K. Michalickova, A. R. Willems, H. Sassi, P. A. Nielsen, K. J. Rasmussen, J. R. Andersen, L. E. Johansen, L. H. Hansen, H. Jespersen, A. Podtelejnikov, E. Nielsen, J. Crawford, V. Poulsen, B. D. Sorensen, J. Matthiesen, R. C. Hendrickson, F. Gleeson, T. Pawson, M. F. Moran, D. Durocher, M. Mann, C. W. V. Hogue, D. Figeys, M. Tyers, Systematic identification of protein complexes in *Saccharomyces cerevisiae* by mass spectrometry. *Nature* **415**, 180–183 (2002).
123. J. Li, G. P. Smith, J. C. Walker, Kinase interaction domain of kinase-associated protein phosphatase, a phosphoprotein-binding domain. *Proc. Natl. Acad. Sci. U.S.A.* **96**, 7821–7826 (1999).
124. J. M. Stone, A. E. Trotochaud, J. C. Walker, S. E. Clark, Control of meristem development by CLAVATA1 receptor kinase and kinase-associated protein phosphatase interactions. *Plant Physiol.* **117**, 1217–1225 (1998).
125. E. R. Morris, D. Chevalier, J. C. Walker, DAWDLE, a forkhead-associated domain gene, regulates multiple aspects of plant development. *Plant Physiol.* **141**, 932–941 (2006).
126. B. Yu, L. Bi, B. Zheng, L. Ji, D. Chevalier, M. Agarwal, V. Ramachandran, W. Li, T. Lagrange, J. C. Walker, X. Chen, The FHA domain proteins DAWDLE in *Arabidopsis* and SNIP1 in humans act in small RNA biogenesis. *Proc. Natl. Acad. Sci. U.S.A.* **105**, 10073–10078 (2008).
127. M. Kim, J.-W. Ahn, K. Song, K.-H. Paek, H.-S. Pai, Forkhead-associated domains of the tobacco NtFHA1 transcription activator and the yeast Fhl1 forkhead transcription factor are functionally conserved. *J. Biol. Chem.* **277**, 38781–38790 (2002).
128. C. J. Bakal, J. E. Davies, No longer an exclusive club: Eukaryotic signalling domains in bacteria. *Trends Cell Biol.* **10**, 32–38 (2000).
129. S. Inouye, R. Jain, T. Ueki, H. Nariya, C. Y. Xu, M. Y. Hsu, B. A. Fernandez-Luque, J. Munoz-Dorado, E. Farez-Vidal, M. Inouye, A large family of eukaryotic-like protein Ser/Thr kinases of *Myxococcus xanthus*, a developmental bacterium. *Microb. Comp. Genomics* **5**, 103–120 (2000).
130. M. Pallen, R. Chaudhuri, A. Khan, Bacterial FHA domains: Neglected players in the phospho-threonine signalling game? *Trends Microbiol.* **10**, 556–563 (2002).
131. A. Telenti, W. J. Philipp, S. Sreevatsan, C. Bernasconi, K. E. Stockbauer, B. Wieles, J. M. Musser, W. R. Jacobs, Jr., The *emb* operon, a gene cluster of *Mycobacterium tuberculosis* involved in resistance to ethambutol. *Nat. Med.* **3**, 567–570 (1997).
132. A. E. Belanger, G. S. Besra, M. E. Ford, K. Mikusova, J. T. Belisle, P. J. Brennan, J. M. Inamine, The embAB genes of *Mycobacterium avium* encode an arabinosyl transferase involved in cell wall arabinan biosynthesis that is the target for the antimycobacterial drug ethambutol. *Proc. Natl. Acad. Sci. U.S.A.* **93**, 11919–11924 (1996).
133. K. G. Papavinasasundaram, B. Chan, J.-H. Chung, M. J. Colston, E. O. Davis, Y. Av-Gay, Deletion of the *Mycobacterium tuberculosis pknH* gene confers a higher bacillary load during the chronic phase of infection in BALB/c mice. *J. Bacteriol.* **187**, 5751–5760 (2005).
134. K. Rittinger, J. Budman, J. Xu, S. Volinia, L. C. Cantley, S. J. Smerdon, S. J. Gamblin, M. B. Yaffe, Structural analysis of 14-3-3 phosphopeptide complexes identifies a dual role for the nuclear export signal of 14-3-3 in ligand binding. *Mol. Cell* **4**, 153–166 (1999).
135. S. M. Pascal, A. U. Singer, T. Yamazaki, L. E. Kay, J. D. Forman-Kay, Structural and dynamic characterization of an SH2 domain-phosphopeptide complex by NMR approaches. *Biochem. Soc. Trans.* **23**, 729–733 (1995).
136. M. A. Verdecia, M. E. Bowman, K. P. Lu, T. Hunter, J. P. Noel, Structural basis for phosphoserine-proline recognition by group IV WW domains. *Nat. Struct. Biol.* **7**, 639–643 (2000).
137. We thank former co-workers and collaborators who have contributed to the work in our laboratory, as well as the colleagues whose papers are cited in this review. We also wish to apologize to colleagues whose studies of the FHA domain may not have been highlighted here. Thanks also go to S. Hsiu-chien Chan for making Fig. 8, A and B. The work from our laboratory was supported by grants from the U.S. National Institutes of Health (CA69472 and CA87031) and the National Health Research Institute of Taiwan (EX95-9508NI).

10.1126/scisignal.151re12

Citation: A. Mahajan, C. Yuan, H. Lee, E. S.-W. Chen, P.-Y. Wu, M.-D. Tsai, Structure and function of the phosphothreonine-specific FHA domain. *Sci. Signal.* **1**, re12 (2008).